

# Automatic Detection of Sleep Apnea Using EEG Signal Based on Modeling of Feature Variation Pattern in Time-Frequency Domains

by  
Arnab Bhattacharjee

Submitted to

Department of Electrical and Electronic Engineering  
in partial fulfillment of the requirements for the degree of  
Master of Science in Electrical and Electronic Engineering


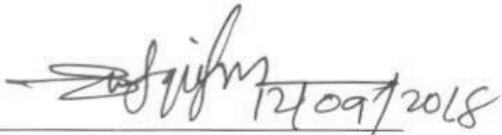
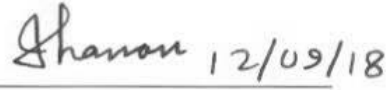
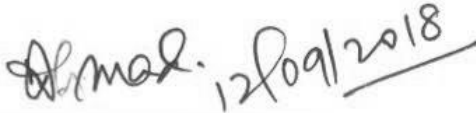


Department of Electrical and Electronic Engineering  
Bangladesh University of Engineering and Technology

Dhaka 1000  
September 2018


The thesis titled “Automatic Detection of Sleep Apnea Using EEG Signal Based on Modeling of Feature Variation Pattern in Time-Frequency Domains”, submitted by Arnab Bhattacharjee, Roll No. 0416062238P, Session April 2016, to the Department of Electrical and Electronic Engineering, Bangladesh University of Engineering and Technology, has been accepted as satisfactory in partial fulfillment of the requirements for the degree of MASTER OF SCIENCE IN ELECTRICAL AND ELECTRONIC ENGINEERING on September 12, 2018.

## Board of Examiners

1.  12.9.18  
Dr. Shaikh Anowarul Fattah  
Professor  
Department of Electrical and Electronic Engineering  
Bangladesh University of Engineering and Technology, Dhaka.  
Chairman  
(Supervisor)
2.  12/09/2018  
Dr. Md. Shafiqul Islam  
Professor and Head  
Department of Electrical and Electronic Engineering  
Bangladesh University of Engineering and Technology, Dhaka.  
Member  
(Ex-Officio)
3.  12/09/18  
Dr. Mohammed Imamul Hassan Bhuiyan  
Professor  
Department of Electrical and Electronic Engineering  
Bangladesh University of Engineering and Technology, Dhaka.  
Member
4.  12/09/2018  
Dr. Mohiuddin Ahmad  
Professor  
Department of Electrical and Electronic Engineering  
Khulna University of Engineering & Technology, Khulna.  
Member  
(External)

# Candidate's Declaration

This is hereby declared that the work titled ‘Automatic Detection of Sleep Apnea Using EEG Signal Based on Modeling of Feature Variation Pattern in Time-Frequency Domains’ is the outcome of research carried out by me under the supervision of Dr. Shaikh Anowarul Fattah, in the Department of Electrical and Electronic Engineering, Bangladesh University of Engineering and Technology, Dhaka 1000. It is also declared that this thesis or any part of it has not been submitted elsewhere for the award of any degree or diploma.

 11/11/18

Arnab Bhattacharjee

Candidate

ID: 0416062238

*Dedicated to my loving parents and my younger brother*

# Acknowledgment

I express my heart-felt gratitude to my supervisor, Dr. Shaikh Anowarul Fattah for his constant supervision of this work. He helped me a lot in every aspect of this work and guided me with proper directions whenever I sought one. He not only acted as my supervisor but also helped me taking important decisions of my academic career. His patient hearing of my ideas, critical analysis of my observations and detecting flaws (and amending thereby) in my thinking and writing have been invaluable. I believe our work in the past one year advanced the state of the art of the sleep apnea detection problem. I also want to thank him for affording so much time for me in exploring new areas of my research and new ideas and improving the writing of this dissertation.

I would also want to thank the members of my thesis committee for their valuable suggestions. I thank Dr. Md. Shafiqul Islam, Dr. Mohammed Imamul Hassan Bhuiyan and specially the external member Dr. Mohiuddin Ahmad. I wish to give special thanks to Dr. Celia Shahnaz, for providing inspiration and guidance to walk in the right path.

In this regard, I remain ever grateful to my parents, my family, without whose prayers and constant support, I could never reach this stage of my life.

# Abstract

Sleep apnea, a serious sleep disorder affecting a large population, causes disruptions in breathing during sleep. For diagnosis, sleep experts manually score the apnea events in overnight polysomnography, which is expensive, tedious, and prone to human error. To counter this problem, in this thesis, an automatic apnea detection scheme is proposed using single lead electroencephalography (EEG) signal, which can discriminate apnea patients and healthy subjects as well as the difficult task of classifying apnea and non-apnea events of an apnea patient. The main theme of the proposed method is to model the within-frame characteristic pattern of a statistical measure of EEG data and use the fitted model parameters as features in apnea detection. For this purpose, within a frame each sub-frame of EEG data is first decomposed and statistical measures, like entropy and log-variance are computed on each decomposed signal. For the purpose of decomposition, frequency domain band-pass filtering, variational mode decomposition and wavelet packet decomposition are considered because of their respective advantages. For a statistical measure, the resulting within-frame variation pattern for each decomposed signal is analyzed and we propose to utilize characteristic probability density function (PDF) to fit the pattern and use the model parameters as features in classifier. Various well known PDFs are investigated and among them the Rician PDF offers very satisfactory feature qualities. For the purpose of classification, the K nearest neighbor classifier is adopted. Extensive experimentation is carried out considering three publicly available large EEG datasets and performance of the proposed method, in comparison to that of the existing methods, is found much superior in terms of sensitivity, specificity and accuracy.

# Contents

<i>Board of Examiners</i>	<b>i</b>
<i>Candidate's Declaration</i>	<b>ii</b>
<i>Acknowledgment</i>	<b>iv</b>
<i>Abstract</i>	<b>v</b>
<b>1 Introduction</b>	<b>1</b>
1.1 Sleep Apnea . . . . .	2
1.2 EEG Signal Analysis . . . . .	4
1.2.1 Source of EEG Signal . . . . .	4
1.2.2 10-20 Standard EEG System . . . . .	5
1.2.3 Band Limited EEG Signals . . . . .	7
1.3 Literature Review . . . . .	10
1.4 Classifier and Classification Schemes . . . . .	13
1.5 Objectives and Scope . . . . .	17
1.6 Organization of the Thesis . . . . .	18
<b>2 Model Based Apnea Detection Using Multi-band EEG Signal</b>	<b>20</b>
2.1 Proposed Method . . . . .	21
2.1.1 Band-limited Signal Extraction . . . . .	22

2.1.2	Multi-band Feature Extraction . . . . .	22
2.1.3	Temporal Feature Variation Pattern Extraction . . . . .	24
2.1.4	Model Fitting of the Extracted Feature Variation Pattern . . . . .	26
2.1.5	Classifier . . . . .	30
2.2	Results and Discussions . . . . .	30
2.2.1	Database . . . . .	31
2.2.2	Goodness of Model Fit . . . . .	33
2.2.3	Feature Quality Test . . . . .	34
2.2.4	Classification Result . . . . .	36
2.3	Conclusion . . . . .	48
<b>3</b>	<b>Model Based Apnea Detection Using Variational Mode Decomposed EEG Signal</b>	<b>50</b>
3.1	Proposed Method . . . . .	51
3.1.1	Analysis with Sub-framing . . . . .	51
3.1.2	Short Description of Variational Mode Decomposition (VMD)	52
3.1.3	Proposed Features for each mode . . . . .	56
3.1.4	Feature Variation Pattern Generation . . . . .	57
3.1.5	Processing of the Extracted Feature Sequence . . . . .	58
3.2	Results and Discussions . . . . .	61
3.2.1	Database . . . . .	61
3.2.2	Feature Quality Test . . . . .	62
3.2.3	Classification Result . . . . .	63
3.3	Conclusion . . . . .	73
<b>4</b>	<b>Model Based Apnea Detection Using Wavelet Packet Decomposed EEG Signal</b>	<b>75</b>
4.1	Proposed Method . . . . .	76



4.1.1	Wavelet Packet Decomposition . . . . .	77
4.1.2	Modeling Analysis of Wavelet Packet Reconstructed Signal .	81
4.2	Results and Discussions . . . . .	84
4.2.1	Database . . . . .	85
4.2.2	Classification Result . . . . .	85
4.3	Conclusion . . . . .	91
<b>5</b>	<b>Conclusion</b>	<b>93</b>
5.1	Concluding Remarks . . . . .	93
5.2	Contribution of this Thesis . . . . .	94
5.3	Scopes for Future Work . . . . .	95

# List of Figures

1.1	Breathing during Normal Breathing and Apnea . . . . .	3
1.2	Sample EEG signals for Apnea and Healthy subjects . . . . .	6
1.3	Different EEG Electrodes . . . . .	7
2.1	Block diagram representing the major steps involved in the proposed method . . . . .	21
2.2	Signals of different EEG sub-bands . . . . .	23
2.3	Sub-framing Operation: a) First Sub-frame b) Second Sub-frame c) Last Sub-frame . . . . .	24
2.4	Variation profile of entropy feature obtained from different band limited EEG signals of test frames (One apnea and one non-apnea frames are considered) . . . . .	25
2.5	Histogram of Sub-frame based feature variation patterns of each sub-band and corresponding Rician fitting . . . . .	28
2.6	Probability Plot for fitting with different PDFs . . . . .	35
2.7	Box plot of model parameters . . . . .	39
2.8	Box plot of statistical parameters . . . . .	39
2.9	Performance criteria with different PDFs . . . . .	40
3.1	Flow chart of the Proposed method . . . . .	51

3.2	Power spectrum densities of $K$ number of VMD modes of an EEG frame (a) $K=3$ (b) $K=4$ (c) $K=5$ (d) $K=6$ . . . . .	55
3.3	Frequency Signature of the Proposed method . . . . .	56
3.4	Entropy feature variation obtained from different IMFs of VMD of both apnea and non-apnea. Here, test frame is divided into multiple sub-frames and each sub-frame is variational mode decomposed. Entropy is calculated from each resulting IMF and the variation profile of with-in frame entropy feature is plotted. . . . .	59
3.5	Histograms of the calculated feature variation patterns and the corresponding Rician fittings of various VMD modes for both apnea and non-apnea frames. . . . .	60
3.6	Distribution of model parameters . . . . .	63
3.7	Variation profile of with-in frame feature is modeled with different PDFs and model parameters are used as input to classifiers. Mean of all the performance criteria are plotted for various PDFs . . . . .	68
3.8	Relative Improvement with the proposed method comparing to the conventional approach. In the conventional approach,unlike sub-frame based analysis, entire frame is used for feature extraction and those are given as inputs directly to the classifier . . . . .	68
3.9	Comparison of Proposed Method with Data Modeling. In data modeling, unlike using the feature variation profile, modeling is applied on the pre-processed EEG data. . . . .	69
3.10	Classification Accuracy with different number of VMD modes taken	70
4.1	Flow chart of the Proposed method . . . . .	76
4.2	Tree decomposition of EEG signal . . . . .	78
4.3	Wavelet packet reconstructed signals at different nodes . . . . .	80

4.4	Test frame is divided into multiple sub-frames and each sub-frame is wavelet packet decomposed. Wavelet coefficients at each node are reconstructed using wavelet packet reconstruction (WPNR). Entropy and log-variance are calculated from each WPNR signal. Histograms of the calculated feature variation patterns of entropy and the corresponding Rician fittings of various WPNR signals are shown for both apnea and non-apnea frames. . . . .	82
4.5	Wavelet packet reconstructed signals at different nodes . . . . .	84
4.6	Classification Result with Various Levels of Decomposition . . . . .	89

# List of Tables

2.1	Definition of Characteristic PDFs . . . . .	29
2.2	Subjects Used For the Evaluation of the Proposed Method . . . . .	32
2.3	Comparison of fitting of different distributions evaluated in Database-A . . . . .	34
2.4	Feature Quality in terms of BC evaluated in Database-A . . . . .	37
2.5	Feature Quality in terms of GSI evaluated in Database-A . . . . .	38
2.6	Definition of Accuracy Measures . . . . .	40
2.7	Classification result of leave-one-out cross validation evaluated in Database-A . . . . .	41
2.8	Classification result of leave-one-out cross validation evaluated in Database-B . . . . .	42
2.9	Classification result of different cross-validation schemes evaluated in Database-A . . . . .	43
2.10	Comparison of the Proposed Method with Other Approaches . . . . .	44
2.11	Comparison of the Proposed Method with the Existing Methods . . . . .	45
2.12	Classification result with all subjects combined . . . . .	46
2.13	Sensitivity of the Proposed Method corresponding to Different Types of Apnea evaluated in Database-A . . . . .	46
2.14	Sensitivity of the Proposed Method Corresponding to Various AHI . . . . .	47
2.15	Performance Comparison Using Different Classifiers . . . . .	48

2.16	Classification result of Apnea and Healthy Data . . . . .	48
3.1	Feature Quality by GSI evaluated in Database-A . . . . .	64
3.2	Performance analysis of the proposed method for various PDF fitting using leave-one-out cross validation (database-A) . . . . .	66
3.3	Performance analysis of the proposed method for various PDF fitting using leave-one-out cross validation (database-B) . . . . .	67
3.4	Effect of model fitting on classification performance (results with and without using the proposed model fitting) . . . . .	70
3.5	Performance Comparison with the Methods Available in Literature	71
3.6	Classification performance with all subjects combined . . . . .	71
3.7	Effect of Position of Electrode in Apnea Detection . . . . .	72
3.8	Performance of the proposed method in classifying apnea and healthy subjects . . . . .	73
4.1	Performance analysis of the proposed method for various PDF fitting using leave-one-out cross validation (database-A) . . . . .	86
4.2	Performance analysis of the proposed method for various PDF fitting (Database-B) . . . . .	87
4.3	Classification performance with all subjects combined of database-A	88
4.4	Comparison of the Proposed method with using Wavelet coefficients for modeling . . . . .	89
4.5	Performance Comparison with the Methods Available in Literature	90
4.6	Performance of the Proposed Method in classifying apnea and healthy subjects . . . . .	90

# Chapter 1

## Introduction

Sleep apnea, a prevalent sleep disorder disrupting sleep quality of the patients, affects about 6-17% of general population where among the elderly, this may be as high as 49% [1]- [2]. Sleep apnea occurs due to obstacle of airflow through the nasal cavity and it causes repetitive cessation of breathing during sleep occur lasting for few seconds to minutes. According to American Academy of Sleep Medicine (AASM) criteria, apnea is scored where reduction in airflow is  $\geq 90\%$  and it stays like so for more than 10 seconds. Patients usually suffer from daytime sleepiness, headaches and various cardio-respiratory disorders due to sleep apnea [3]-[4]. Sleep apnea may increase the risk of heart attack, stroke, diabetes, heart failure, irregular heartbeat, obesity, and motor vehicle collisions.

The study of overnight polysomnography (PSG) is a standard method for sleep apnea diagnosis. In this method, a patient spends the whole night in an observation room and several accessible bio-signals, such as Electroencephalography (EEG), electromyography (EMG), electrocardiogram (ECG), electroculogram (EOG), oro-nasal airflow, ribcage movements, abdomen movements (uncalibrated strain gauges), oxygen saturation (finger pulse oximeter) and snoring (tracheal microphone) are collected. With the help of collected bio-signals, expert scores the

apnea events manually. Visual identification of sleep apnea events with the help of a sleep expert is expensive, time consuming, laborious and erroneous. In some cases, a very small duration of apnea (10-20 sec) may occur after a long interval (1 or 2 hours) and the observer may miss it. Hence, it is of great necessity to develop an algorithm for automatic apnea detection.

## 1.1 Sleep Apnea

Sleep apnea is a sleep disorder characterized by pauses in breathing or periods of shallow breathing during sleep. Each pause can last for a few seconds to a few minutes and such pauses happen many times a night. In the most common form, sleep apnea causes loud snoring. There may be a choking or snorting sound as breathing resumes. As the disorder disrupts normal sleep, those affected may experience sleepiness or feel tired during the day. In children it may cause problems in school, or hyperactivity. It affects males about twice as often as females. While people at any age can be affected, it occurs most commonly among those 55 to 60 years old. Figure 1.1 shows breathing during normal condition and apnea. It is observed that during apnea the airway gets almost blocked thus a disruption in breathing is caused.

There are three forms of sleep apnea: obstructive sleep apnea (OSA), central sleep apnea (CSA), and a combination of the two called mixed. The OSA is the most common form. Risk factors for the OSA include being overweight, allergies, a small airway, and enlarged tonsils. In OSA, breathing is interrupted by a blockage of airflow, while in CSA breathing stops due to a lack of effort to breathe. People with sleep apnea may not be aware of having this disease. In many cases, it is first observed by a family member. Sleep apnea is often diagnosed with an overnight sleep study. For a diagnosis of sleep apnea, more than five occurrences



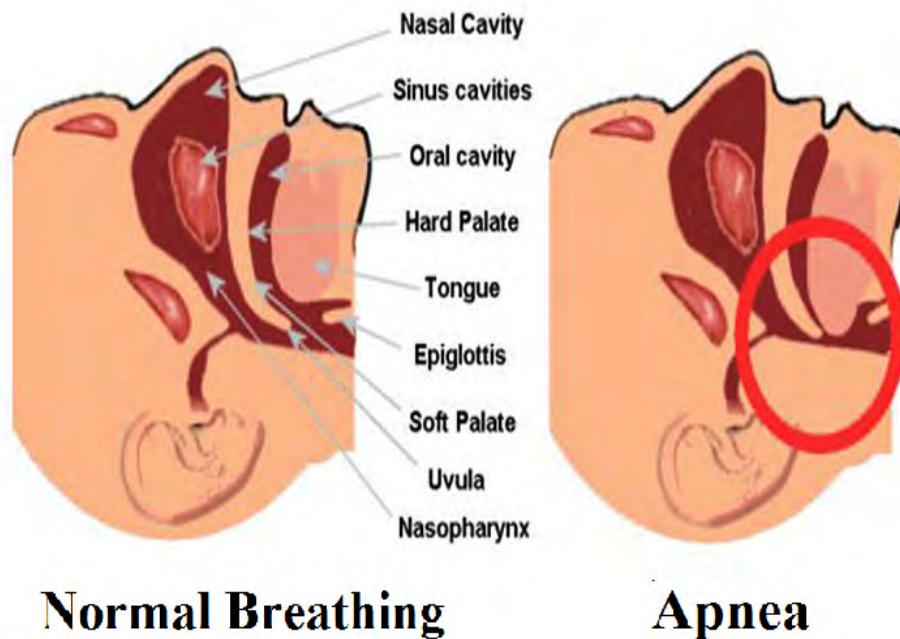


Figure 1.1: Breathing during Normal Breathing and Apnea

an hour must occur. Central sleep apnea affects less than 1% of people. People with sleep apnea have problems with excessive daytime sleepiness (EDS), impaired alertness, and vision problems. OSA may increase risk for driving accidents and work-related accidents. If OSA is not treated, people are at increased risk of other health problems, such as diabetes. Death could occur from untreated OSA due to lack of oxygen to the body. Without treatment, sleep apnea may increase the risk of heart attack, stroke, diabetes, heart failure, irregular heartbeat, obesity, and motor vehicle collisions.

Treatment may include lifestyle changes, mouthpieces, breathing devices, and surgery. Lifestyle changes may include avoiding alcohol, losing weight, stopping smoking, and sleeping on one's side. Breathing devices include the use of a Continuous positive airway pressure (CPAP) machine.

## 1.2 EEG Signal Analysis

An EEG is a process used to evaluate the electrical activity in the brain. Brain cells communicate with each other through electrical impulses. An EEG can be used to help detecting this activity. During EEG recordings, small sensors are attached to the scalp to pick up the electrical signals produced when brain cells send messages to each other. These signals are recorded by a machine and can be utilized to establish communication between man and machine. Since this recording process is non-invasive i.e. the electrode only picks up electric signal from the brain and does not affect the brain. Therefore, this process is totally painless and harmless. Despite limited spatial resolution, EEG continues to be a valuable tool for research and diagnosis, especially when millisecond-range temporal resolution is required.

### 1.2.1 Source of EEG Signal

EEG is a graphic representation of the difference in voltage between two different cerebral locations plotted over time. The scalp EEG signal generated by cerebral neurons is modified by electrical conductive properties of the tissues between the electrical source and the recording electrode on the scalp, conductive properties of the electrode itself, as well as the orientation of the cortical generator to the recording electrode. Because of the process of current flow through the tissues between the electrical generator and the recording electrode which is known as volume conduction, EEG provides a two-dimensional projection of our brain. It detects the summed ionic currents of thousands of pyramidal neurons beneath each of the 16 and 25 individual macro electrodes, and reports them as voltage differences across low resistance extracellular space. Specifically, the potentials recorded by the macro-electrodes on the skin of the skull are primarily generated by extracellular current flow of synaptic potentials in pyramidal cells. Action potentials of

the neurons are usually asynchronous and too fast-moving to generate detectable potentials on the skin's surface. As a result, brain cells other than pyramidal neurons such as interneurons and glial cells make relatively little contribution to skin potentials because, unlike pyramidal neurons, these cells are neither oriented in parallel to one another nor do their dendrites run perpendicular to the cortical surface. In contrast, pyramidal neurons run parallel to one another with large dendritic branches that run perpendicular to the cortical surface. Since voltage fields fall off with the square of distance, activity from deep sources is more difficult to detect than currents near the skull. The EEG waves obtained from the scalp electrodes show oscillations at different frequencies. Such oscillations at a variety of frequencies are associated with different states of brain functioning involving different parts of our brain. As a result, such oscillations depict synchronized activity over different networks of neurons which are known as neuronal networks. From such neuronal networks some of these oscillations are understood, while many others are not. Figure 1.2 shows sample EEG signals for Apnea and Healthy subjects. It is to be seen that through visual inspection it is very difficult to differentiate between the two classes.

### **1.2.2 10-20 Standard EEG System**

The international 10-20 system of electrode placement is the most widely used method to describe the location of scalp electrodes during an EEG recording or experiment. The 10-20 system is based on the relationship between the location of an electrode and the underlying area of cerebral cortex. Each site has a letter (to identify the lobe) and a number or another letter to identify the hemisphere location. The positions of the electrodes of the 10-20 system are shown in Fig. 1.3. This method was developed to ensure standardized reproducibility so that a subjects studies could be compared over time and subjects could be compared

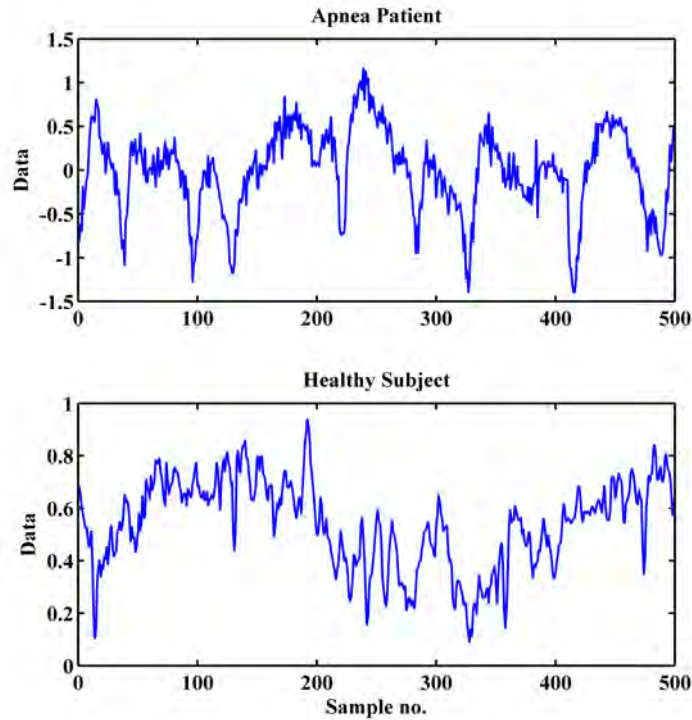


Figure 1.2: Sample EEG signals for Apnea and Healthy subjects

to each other. The letters F, T, C, P and O stand for frontal, temporal, central, parietal, and occipital lobes, respectively. Even numbers (2, 4, 6, and 8) refer to the right hemisphere and odd numbers (1, 3, 5 and 7) refer to the left hemisphere. "Z" refers to an electrode placed on the mid line. The smaller the number, the closer the position to the mid line. "Fp" stands for Front polar. Two anatomical landmarks are used for the essential positioning of the EEG electrodes: first, the nasion which is the point between the forehead and the nose; second, the inion which is the lowest point of the skull from the back of the head and is normally indicated by a prominent bump. The "10" and "20" (10-20 system) refer to the 10% and 20% inter electrode distance. When recording a more detailed EEG with more electrodes, extra electrodes are added utilizing the spaces in-between the existing 10-20 system. This new electrode-naming-system is more complicated giving rise

to the Modified Combinatorial Nomenclature (MCN). This MCN system uses 1, 3, 5, 7, 9 for the left hemisphere which represents 10%, 20%, 30%, 40%, 50% of theinion-to-nasion distance respectively. 2, 4, 6, 8, 10 are used to represent the right hemisphere. The introduction of extra letters allows the naming of extra electrode sites. These new letters do not necessarily refer to an area on the underlying cerebral cortex.

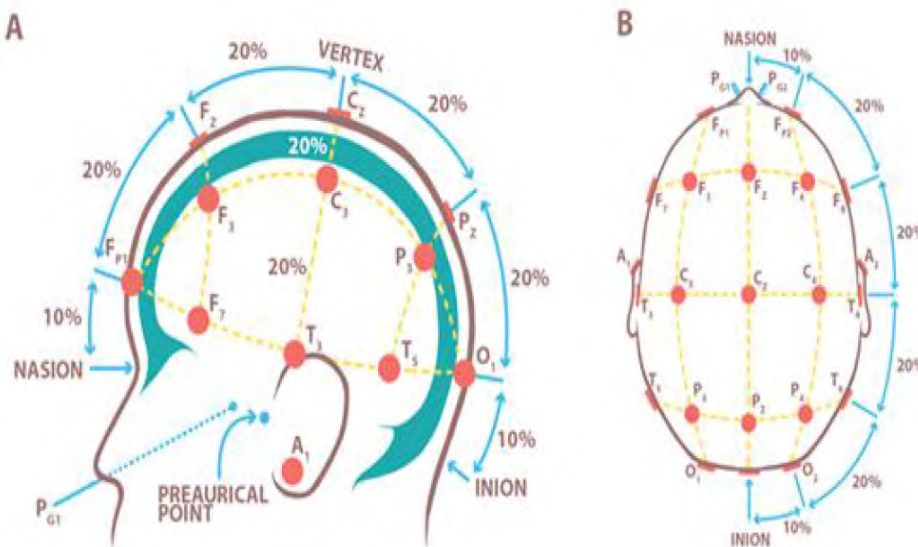


Figure 1.3: Different EEG Electrodes

### 1.2.3 Band Limited EEG Signals

It is important to know that humans display five different types of EEG signal. Each brain wave has a purpose and helps serve us in optimal mental functioning. Each serves a purpose to help us cope with various situations – whether it is to help us process and learn new information or help us calm down after a long stressful day. The five brain waves in order of lowest frequency to highest are as follows: delta, theta, alpha, beta and gamma.

**Delta wave** Delta waves are associated with deep levels of relaxation and restorative sleep. They are the slowest recorded brain waves in humans and higher levels are more commonly found in young children. During the aging process, lower Delta waves are produced. Research tells us that Delta waves are attributed to many of our unconscious bodily functions such as regulating the cardiovascular and the digestive systems. Healthy levels of Delta waves can contribute to a more restful sleep, allowing us to wake up refreshed, however irregular delta wave activity has been linked to learning difficulties or issues maintaining awareness.

Frequency range: 0 Hz to 4 Hz, High levels: Brain injuries, learning problems, inability to think, severe ADHD, Low levels: Inability to rejuvenate body, inability to revitalize the brain, poor sleep, Optimal range: Healthy immune system, restorative REM sleep.

**Theta wave** Theta waves known as the ‘suggestible waves’, because of their prevalence when one is in a trance or hypnotic state. In this state, a brain’s Theta waves are optimal and the patient is more susceptible to hypnosis and associated therapy. The reasoning for this is that Theta waves are commonly found when you daydream or are asleep, thus exhibiting a more relaxed, open mind state. Theta waves are also linked to us experiencing and feeling deep and raw emotions, therefore too much theta activity may make people prone to bouts of depression. Theta does however has its benefits of helping improve our creativity, wholeness and intuition, making us feel more natural. It is also involved in restorative sleep and as long as theta isn’t produced in excess during our waking hours, it is a very helpful brainwave range.

Frequency range: 4 Hz to 8 Hz, High levels: ADHD or hyperactivity, depressive states, impulsive activity or inattentiveness, Low levels: Anxiety symptoms, poor emotional awareness, higher stress levels, Optimal range: Maximum creativity,

deep emotional connection with oneself and others, greater intuition, relaxation.

**Alpha wave** Alpha waves are the ‘frequency bridge’ between our conscious thinking (Beta) and subconscious (Theta) mind. They are known to help calm you down and promote feelings of deeper relaxation and content. Beta waves play an active role in network coordination and communication and do not occur until three years of age in humans. In a state of stress, a phenomenon called ‘Alpha blocking’ can occur which involves excessive Beta activity and little Alpha activity. In this scenario, the Beta waves restrict the production of alpha because we because our body is reacting positively to the increased Beta activity, usually in a state of heightened cognitive arousal.

Frequency range: 8 Hz to 12 Hz, High levels: Too much daydreaming, over-relaxed state or an inability to focus, Low levels: OCD, anxiety symptoms, higher stress levels, Optimal range: Ideal relaxation.

**Beta Waves** Beta waves are the high frequency waves most commonly found in awake humans. They are channeled during conscious states such as cognitive reasoning, calculation, reading, speaking or thinking. Higher levels of Beta waves are found to channel a stimulating, arousing effect, which explains how the brain will limit the amount of Alpha waves if heightened Beta activity occurs. However, if you experience too much Beta activity, this may lead to stress and anxiety. This leads you feeling overwhelmed and stressed during strenuous periods of work or school. Beta waves increased by drinking common stimulants such as caffeine or L-Theanine, or by consuming Nootropics or cognitive enhancers such as Lucid.

Frequency range: 12 Hz to 40 Hz, High levels: Anxiety, inability to feel relaxed, high adrenaline levels, stress, Low levels: Depression, poor cognitive ability, lack of attention, Optimal range: Consistent focus, strong memory recall, high problem solving ability.

**Gamma wave** Gamma waves are a more recent discovery in the field of neuroscience, thus the understanding of how they function is constantly evolving. To date, it's known that Gamma waves are involved in processing more complex tasks in addition to healthy cognitive function. Gamma waves are found to be important for learning, memory and processing and they are used as a binding tool for our senses to process new information. In people with mental disabilities, much lower levels of Gamma activity is recorded. More recently, people have found a strong link between meditation and Gamma waves, a link attributed to the heightened state of being or 'completeness', experienced when in a meditative state.

Frequency range: 40 Hz to 100 Hz, High levels: Anxiety, stress, Low levels: Depression, ADHD, learning issues, Optimal range: Information processing, cog-nition, learning, binding of senses.

### 1.3 Literature Review

EEG signal is getting special attention by the researchers in analyzing sleep related problems as it has direct relevance with neural activity. There are many automatic sleep apnea detection methods available in literature, however, most of them utilize multiple biomedical signals including EEG. For example, in [5], oxygen saturation, heart rate variability and the respiratory signals, in [6], EOG, EMG, heart rate variability, oronasal temperature, nasal pressure, in [7] oximetric signal, in [8] pupil size, in [9] EMG signal and in [10] EOG, EMG, ECG signals are utilized. However, use of multiple (or multi-channel) bio-signals has several disadvantages, such as cost of additional sensors, discomfort for the patient, excessive data acquisition and processing requirement and computational expense in terms of time and implementation. Hence apnea detection with a single channel bio-signal is of great necessity. The advancement in wearable EEG data acquisi-



tion system has opened up a new direction for various EEG based disease analysis and thus apnea detection from EEG signal is now getting special attention by the researchers [11]-[22].

In [11], detrended fluctuation analysis (DFA) is used to compute EEG scaling exponents which are utilized as features for classifying apnea and healthy subjects. Here, 30 min EEG scaling exponents that quantify powerlaw correlations were computed using DFA and compared between six sleep apnea subjects (SAS) and six healthy subjects. The mean scaling exponents were calculated every 30s and 360 control values and 360 apnea values were obtained during sleep.

In [12]- [13], wavelet analysis is employed on EEG data to identify sleep apnea events. In [12], EEG signals are separated into delta, theta, alpha, and beta spectral components by using multi-resolution discrete wavelet transforms (DWT). These spectral components are applied to the inputs of the artificial neural network where the wavelet coefficients are treated as the the training input of artificial neural network. The neural network is configured to obtain differentiable outputs to signify the sleep apnea patient. In [13], EEG signals are decomposed by four level wavelet transform to obtain the CD4 wavelet coefficients which are used as input for the GreyART (Grey relational analysis and Adaptive resonant theory) network. The GreyART network was then used for simulation training and testing purpose.

In [14], particle swarm optimization based hermite decomposition algorithm is proposed. The information from randomly varying complex EEG signals is extracted in terms of PSO optimised Hermite functions (HFs), with constraint of minimum error function. The Hermite coefficients computed from HFs-based statistical features are applied as input to PSO parameterised least square support vector machine classifier. The proposed decomposition for EEG signals provides negligible mean value of error function and obtains satisfactory apnea identification

result.

Instead of using the full band EEG signal, an effective way is to divide the EEG signal into well-known EEG sub-bands and analyze the band limited signals. But for band limited signal extraction bandpass filters with fixed bandwidth are used whereas neural activity varies from time to time, person to person. Hence, the possible benefits in analysis with the use of adaptive bandwidth based decomposition for band limited signal extraction is yet to be explored. Recently in [15], sub-frame based features are modeled for band limited signals, where the signals are obtained by simple bandpass filtering. However, in the method the effect of including higher frequency bands ( $>40\text{Hz}$ ) in apnea detection is not considered. In [16], for apnea classification, energy and variance are computed from each sub-band. In [17], random characteristics of EEG signal is exploited by multi-band entropy values to use as features while in [18], cumulative delta-power ratio of overlapping frames is used. Variation of within frame EEG beta band energy is studied and various statistical features are extracted from the energy variation pattern in [19].

In [20], intrinsic mode functions (IMF) of empirical mode decomposed EEG signal are separated into amplitude modulated (AM) and frequency modulated (FM) components using Teager energy operator which are used for feature extraction. The extracted features from separated components are applied as input to least square support vector machine (LS-SVM) classifier. Bispectral characteristics of EEG signal are investigated in [21]. Bispectral analysis is an advanced signal processing technique particularly used for exhibiting Quadratic phase coupling (QPC) that may arise between signal components with different frequencies. The amount of QPC in each sub-band of EEG (namely; delta, theta, alpha, beta and gamma) was calculated over bispectral density of EEG. Then, these QPCs were fed to the input of the designed ANN

In [22], variation of Hilbert spectrum frequency is studied. It extracts frequency elements from Hilbert spectrum by Hilbert–Huang transformation. The system then detects duration of obstructive sleep apnea from the variation of Hilbert spectrum frequency. The main contribution of the system is to preserve time information in the electroencephalogram by Hilbert–Huang transformation mechanism as well as find frequency variation information. The system also allows free adjustment of time scale to establish a flexible detection system with fast response so it is capable of real time detection of obstructive sleep apnea.

However, most of the methods reported above, classify between apnea and healthy subjects and the challenging task of differentiating apnea and non-apnea frames of an apnea patient is not much investigated.

## 1.4 Classifier and Classification Schemes

classification is the problem of identifying to which of a set of categories (sub-populations) a new observation belongs, on the basis of a training set of data containing observations (or instances) whose category membership is known. Classifier is an algorithm that implements classification, especially in a concrete implementation, is known as a classifier. The term "classifier" sometimes also refers to the mathematical function, implemented by a classification algorithm, that maps input data to a category. There are various types of classifier. In the following brief introductions of few classifiers are provided.

**K-NN Classifier** K-nearest neighbors algorithm (K-NN) is a non-parametric method used for classification and regression. In both cases, the input consists of the K closest training examples in the feature space. The output depends on whether K-NN is used for classification or regression:

i) In K-NN classification, the output is a class membership. An object is classified by a majority vote of its neighbors, with the object being assigned to the class most common among its K nearest neighbors (K is a positive integer, typically small). If  $K = 1$ , then the object is simply assigned to the class of that single nearest neighbor.

ii) In K-NN regression, the output is the property value for the object. This value is the average of the values of its k nearest neighbors.

K-NN is a type of instance-based learning, or lazy learning, where the function is only approximated locally and all computation is deferred until classification. The K-NN algorithm is among the simplest of all machine learning algorithms.

Both for classification and regression, a useful technique can be used to assign weight to the contributions of the neighbors, so that the nearer neighbors contribute more to the average than the more distant ones. For example, a common weighting scheme consists in giving each neighbor a weight of  $1/d$ , where d is the distance to the neighbor.

The neighbors are taken from a set of objects for which the class (for K-NN classification) or the object property value (for K-NN regression) is known. This can be thought of as the training set for the algorithm, though no explicit training step is required.

**SVM Classifier** Support vector machines (SVMs) are supervised learning models with associated learning algorithms that analyze data used for classification and regression analysis. Given a set of training examples, each marked as belonging to one or the other of two categories, an SVM training algorithm builds a model that assigns new examples to one category or the other, making it a non-probabilistic binary linear classifier. An SVM model is a representation of the examples as points in space, mapped so that the examples of the separate categories are di-

vided by a clear gap that is as wide as possible. New examples are then mapped into that same space and predicted to belong to a category based on which side of the gap they fall.

In addition to performing linear classification, SVMs can efficiently perform a non-linear classification using what is called the kernel trick, implicitly mapping their inputs into high-dimensional feature spaces. There are several kernels of which polynomial, RBF kernels are mostly used.

**LDA Classifier** LDA is also closely related to principal component analysis (PCA) and factor analysis in that they both look for linear combinations of variables which best explain the data. LDA explicitly attempts to model the difference between the classes of data. LDA works when the measurements made on independent variables for each observation are continuous quantities. When dealing with categorical independent variables, the equivalent technique is discriminant correspondence analysis.

Discriminant analysis is used when groups are known a priori (unlike in cluster analysis). Each case must have a score on one or more quantitative predictor measures, and a score on a group measure. In simple terms, discriminant function analysis is classification - the act of distributing things into groups, classes or categories of the same type.

**Artificial Neural Network** Artificial neural networks (ANN) are computing systems vaguely inspired by the biological neural networks that constitute animal brains. Such systems "learn" to perform tasks by considering examples, generally without being programmed with any task-specific rules. An ANN is based on a collection of connected units or nodes called artificial neurons which loosely model the neurons in a biological brain. Each connection, like the synapses in a biological brain, can transmit a signal from one artificial neuron to another. An artificial

neuron that receives a signal can process it and then signal additional artificial neurons connected to it.

In common ANN implementations, the signal at a connection between artificial neurons is a real number, and the output of each artificial neuron is computed by some non-linear function of the sum of its inputs. The connections between artificial neurons are called ‘edges’. Artificial neurons and edges typically have a weight that adjusts as learning proceeds. The weight increases or decreases the strength of the signal at a connection. Artificial neurons may have a threshold such that the signal is only sent if the aggregate signal crosses that threshold. Typically, artificial neurons are aggregated into layers. Different layers may perform different kinds of transformations on their inputs. Signals travel from the first layer (the input layer), to the last layer (the output layer), possibly after traversing the layers multiple times.

The original goal of the ANN approach was to solve problems in the same way that a human brain would. However, over time, attention moved to performing specific tasks, leading to deviations from biology. Artificial neural networks have been used on a variety of tasks, including computer vision, speech recognition, machine translation, social network filtering, playing board and video games and medical diagnosis.

**Cross-validation Schemes** Cross-validation is one of various similar model validation techniques for assessing how the results of a statistical analysis will generalize to an independent data set. It is mainly used in settings where the goal is prediction, and one wants to estimate how accurately a predictive model will perform in practice. In a prediction problem, a model is usually given a dataset of known data on which training is run (training dataset), and a dataset of unknown data (or first seen data) against which the model is tested (called the validation

dataset or testing set). The goal of cross-validation is to test the model's ability to predict new data that was not used in estimating it, in order to flag problems like overfitting and to give an insight on how the model will generalize to an independent dataset (i.e., an unknown dataset, for instance from a real problem).

In K Fold cross validation, the data is divided into k subsets. Now the classification is repeated k times, such that each time, one of the k subsets is used as the test set/ validation set and the other k-1 subsets are put together to form a training set. The error estimation is averaged over all k trials to get total effectiveness of our model. As can be seen, every data point gets to be in a validation set exactly once, and gets to be in a training set k-1 times. This significantly reduces bias as we are using most of the data for fitting, and also significantly reduces variance as most of the data is also being used in validation set. Interchanging the training and test sets also adds to the effectiveness of this method.

## 1.5 Objectives and Scope

The objectives of the thesis are:

- i) To develop sub-frame based temporal feature variation pattern by extracting statistical features from EEG data in time-frequency, variational mode decomposition (VMD) and wavelet packet decomposition (WPD) domain.
- ii) To model the feature variation pattern with conventional probability distribution functions (PDFs) and use characteristic parameters of the fitted PDF as feature.
- iii) To investigate the quality of the proposed feature vector in terms of class separability by the standard goodness of feature measures.
- iv) To validate the performance of the proposed method by conducting experiments on three publicly available EEG sleep datasets.

The scope of this thesis will be a computationally efficient method of automatic sleep apnea detection from single channel EEG signal, which will make diagnosis of patients easy and human error free.

## 1.6 Organization of the Thesis

In the first Chapter, a definition of sleep apnea disease, its current statistics all around the world, its symptoms- adverse affects and the current diagnosis system are presented. For the purpose of automating the detection process the feasibility and motivation behind using single channel EEG signal is discussed and data acquisition technique of EEG signal is presented. Moreover, the Chapter provides the motivation and objectives of the thesis by presenting the past and current research scenarios of sleep apnea detection. The rest of the thesis is organized as follows.

In Chapter 2, a model based apnea detection scheme is proposed where sub-frame based feature variation patterns have been modeled in multi-band EEG signal, where the bands correspond to traditional EEG bands used in literature. The multi-band EEG signals are divided into a number of sub-frames and statistical features those are believed to be have the potential to apnea and non-apnea are calculated from each sub-frame. Next, within frame feature variation patterns for each band corresponding to the features used are generated. These feature variation patterns are statistically analyzed and are fitted with probabilistic model and the statistical and fitted model parameters are used as features to classify apnea and non-apnea. K-NN classifier is used for classification and extensive experimentations have been carried out in three different publicly available databases.

In Chapter 3, Variational mode decomposition analysis is carried out for apnea



detection. Here, sub-framed EEG data are variational mode decomposed and statistical features are extracted from each mode. As like Chapter 2, feature variation patterns are generated for each mode and the patterns are further subjected to statistical and modeling analysis. K-NN classifier is used where statistical and fitted model parameters are used as inputs. Detail experimental results are presented for the same databases.

In Chapter 4, wavelet packet reconstruction has been utilized in sub-framed EEG signal and features are extracted from the reconstructed signals at different nodes. Next, As like Chapter 2, feature variation patterns are generated for each node and statistical and modeling analyses are carried out of these patterns to form the final feature vector. Classification is carried out using K-NN classifier. Detail experimental results are presented considering the same dataset.

Chapter 5 summarizes the outcome of this thesis with some concluding remarks and possible future works.

## Chapter 2

# Model Based Apnea Detection Using Multi-band EEG Signal

In this Chapter, a sub-frame based model fitting approach is proposed where both the classification scenarios, classification between apnea and healthy subjects as well as the task of discriminating apnea and non-apnea events in the data of an apnea patient, are taken into consideration. First, a multi-band sub-frame based scheme is introduced to extract the feature variation pattern within a frame. Next, the feature variation patterns are processed using statistical analysis and modeled with characteristic probability density function. Resulting model parameters and some statistical measures are used in K nearest neighbor (K-NN) classifier to classify apnea and non-apnea frames. Detail experimentations and performance analyses are carried out in three different publicly available databases. The uniqueness of the proposed method lies in modeling the within-frame feature variation pattern and utilizing the fitted model parameters as potential features in the classification scheme, which offers very low feature dimension. Unlike using multiple bio-signals, this paper focuses on automatic detection of sleep apnea using single lead EEG signal which makes the system cost effective and can lead to an auto-diagnostic

device favorable for in-home care. Outcome of this research has been reported in [15].

## 2.1 Proposed Method

The major steps involved in the proposed method are illustrated in Fig. 2.1. A given frame of raw EEG data is first pre-processed, divided into frequency bands, and then proposed sub-frame based feature extraction scheme is employed in each band-limited signal. Finally statistical analysis and modeling are applied to extract the feature vector to be used in the classifier. In what follows, detailed description of each step is presented.

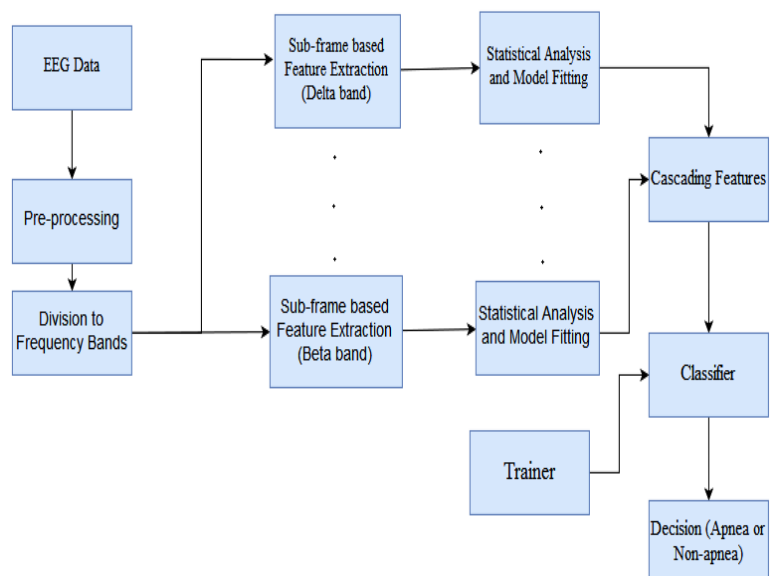


Figure 2.1: Block diagram representing the major steps involved in the proposed method

### 2.1.1 Band-limited Signal Extraction

DC offset of a frame of EEG data is removed followed by frame amplitude normalization. During sleep activity level of recorded EEG data changes as the mental state and the sleep stage continuously change with respect to time. As a result, there is a large change in energy content in different EEG frames. Energy normalization is carried out in each frame to counter this phenomena.

EEG signal exhibits significantly different characteristics in different frequency bands. During apnea, carbon dioxide builds up in the bloodstream as breathing is paused, which is identified by the chemoreceptors and brain signals the person sleeping to wake up and breathe in air [23]. Such changes in neural activity level from non-apnea to apnea can cause notable variation in various frequency bands of the EEG data, namely: delta(0.25-4 Hz), theta(4-8 Hz), alpha(8-12 Hz), sigma(12-16 Hz) and beta(16-40 Hz). In the proposed method, five band-pass filters are used to extract the band limited EEG signals which are expected to preserve local information better with respect to full band signal. Figure 2.2 shows an example of different signals EEG sub-bands.

### 2.1.2 Multi-band Feature Extraction

For a band limited EEG data, among various statistical features, entropy and log-variance are used in the proposed method. Entropy of a discrete random variable  $Y$  with possible values  $\{y_0, y_1, y_2, \dots, y_M\}$  is defined as

$$H(Y) = - \sum_{i=0}^M p(y_i) \times \log_2(p(y_i)) \quad (2.1)$$

where  $p(y_i) = n_i/N$ , with  $n_i$  be the number of occurrence corresponding to  $y_i$  value among the  $N$  number of values, i.e.  $\sum_i n_i = N$ . During apnea, normal breathing is hampered and patient may make gasping, grunting or snorting sounds

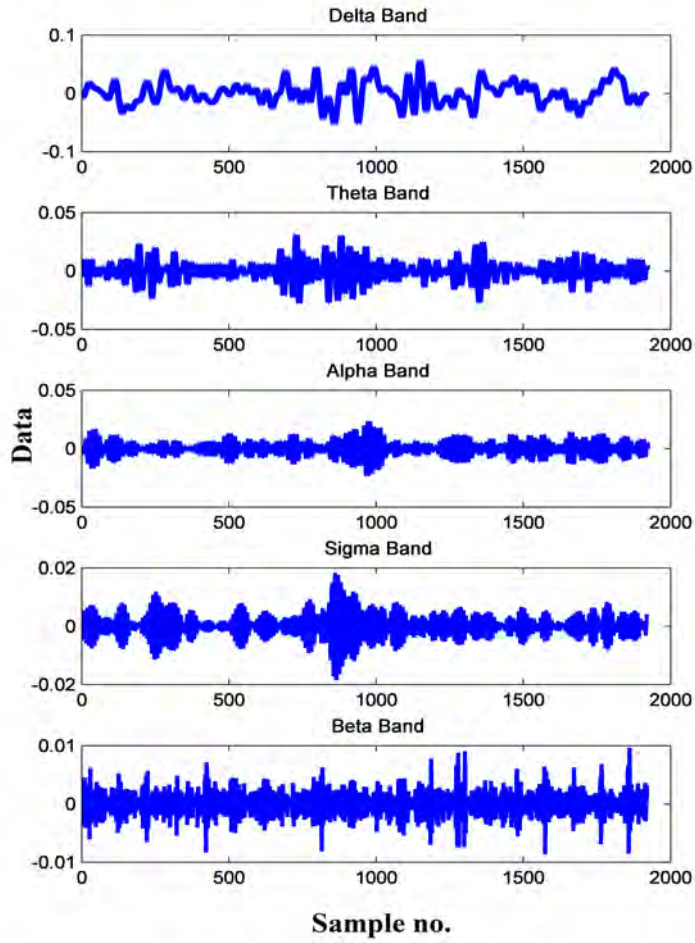


Figure 2.2: Signals of different EEG sub-bands

and restless body movements. Since EEG signal contains information regarding different mental and motor-imagery states of the brain, it is expected that for a person at sleep, during apnea events there will be certainly a rapid change in information content in EEG recordings. As entropy is a statistical measure of information content, it is proposed as a potential feature for apnea event detection. For an  $N$  length EEG data  $s[n]$  with mean value  $\mu$ , log-variance (LV) is expressed as

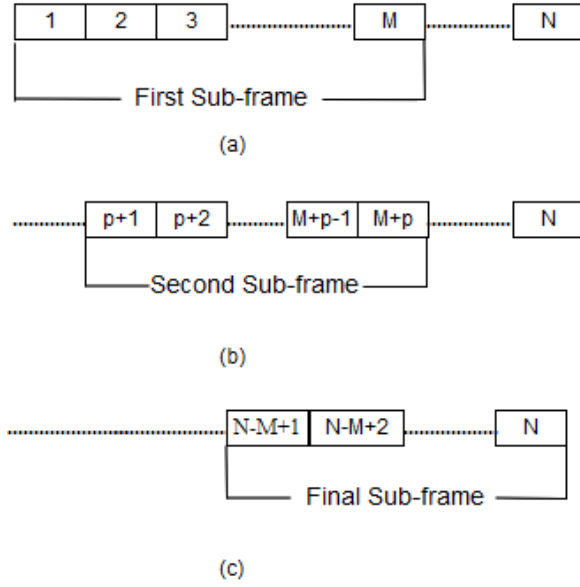


Figure 2.3: Sub-framing Operation: a) First Sub-frame b) Second Sub-frame c) Last Sub-frame

$$LV = \log_e \left[ \frac{1}{N} \sum_{n=1}^N (s[n] - \mu)^2 \right]. \quad (2.2)$$

Similarly, it is expected that variance of EEG signal would be different in both the classes. As variance of EEG is very small, logarithm of variance is used.

### 2.1.3 Temporal Feature Variation Pattern Extraction

In frame by frame analysis, generally the whole duration of a test frame is considered for feature extraction. As an alternate, dividing a frame into overlapping short duration sub-frames offers an advantage of capturing precisely local signal characteristics. In an  $N$  length signal with sub-frame length  $M$ , shifting by  $p$  samples with  $p \ll M < N$ , there will be a total  $\frac{N-M}{p} + 1$  number of sub-frames. Figure 2.3 shows the procedure of sub-frame operation.

If a particular feature is extracted from each sub-frame, a temporal profile of that feature within a frame can be obtained and the properties of that sub-frame based feature sequence can be utilized. A major advantage of using sub-frame based feature extraction is the reduction of the effect of random fluctuation in a given test frame. For example, an unexpected value in a test frame can significantly affect the overall feature value. However, in sub-frame based analysis that unexpected value will affect only a mere portion of the total sub-frames. Thus overall analysis carried out using sub-frame based feature values can provide better characteristics of a test frame in comparison to the case where features are calculated using whole test frame. Another key factor is that not the entire N

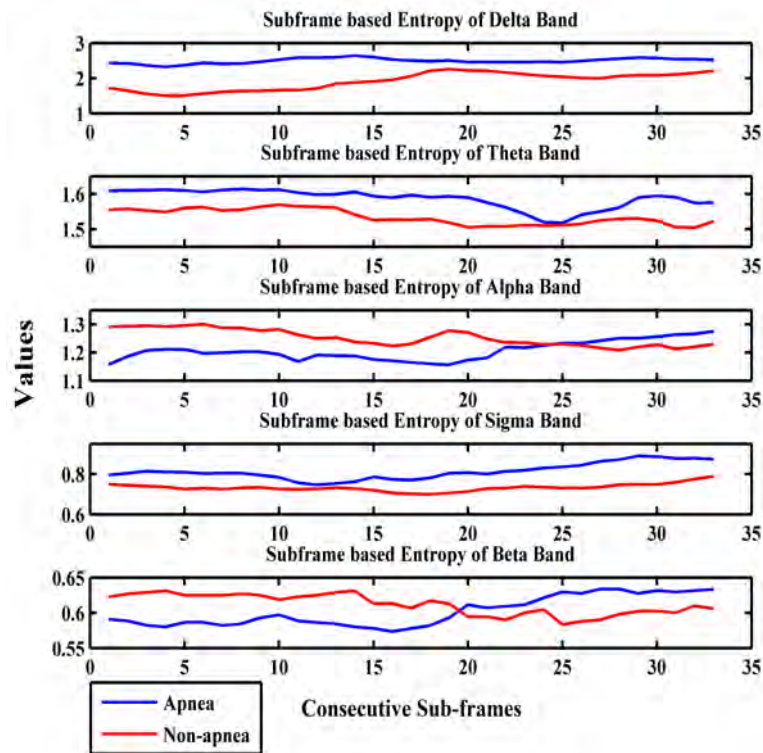


Figure 2.4: Variation profile of entropy feature obtained from different band limited EEG signals of test frames (One apnea and one non-apnea frames are considered)

samples of a particular frame correspond to an apneic zone as frame duration is taken higher than the typical apnea duration. Apnea may occur only for a limited period in the whole duration of frame. Sub-framing increases the probability of correctly identifying the particular apneic event since sub-frame based extracted features exhibit sharp changes in its characteristics within an apnea frame, in particular at the transition between apnea and non-apnea events. Considering reasonably large frame size, where apnea duration is less than a frame duration, it is obvious that a transition will exist either from apnea to non-apnea or from non-apnea to apnea or both. Feature extracted from the entire frame at a time, may not be able to characterize such changes.

In order to demonstrate the variation of a feature within a frame in sub-frame based analysis, in Fig. 2.4, entropy feature patterns extracted from each band limited signal are presented. Here two frames, one apnea and one non-apnea are considered. It is clearly observed from the figure that in different band limited signals, characteristics of the extracted feature patterns differ significantly between apnea to non-apnea cases.

#### **2.1.4 Model Fitting of the Extracted Feature Variation Pattern**

Characteristic profile of a particular feature obtained from sub-frame based analysis can directly be used as feature for classifying a test frame. However, direct use of the feature sequence involves large feature dimension. As an alternate, efficient processing schemes can be applied on the feature variation pattern to extract distinct information for the purpose of classifying apnea and non-apnea events. One possible way is to extract various statistical features of feature variation pattern. Among different statistical features, mean and variance are considered in the proposed method. In addition to that, with the purpose of quantifying the



variation pattern of sub-frame based extracted features, characteristics its amplitude variation can be investigated. In this work, it is proposed to fit the sub-frame based extracted feature sequences with characteristic probability density functions (PDFs). The idea is to fit sub-frame based feature variation with a PDF and then use the fitted model parameters as feature. In this case, most of the well known PDFs can be taken into consideration, such as Gaussian, Exponential, Rayleigh etc. Description of different popular PDFs is given in Table 2.1 [24]. This approach will provide an opportunity to capture the variations of statistics of data distributions in apnea and non-apnea. As the number of characteristic parameters is small (most of the cases one or two), feature dimension would be drastically reduced in comparison to using the whole sub-frame based feature sequence. Out of several PDFs, in this work, we propose to use Rician PDF to fit the feature variation pattern. Detailed analysis using different PDFs is followed in Section 2.2 in this Chapter. The histograms of feature sequences and corresponding Rician fitting of several apnea and non-apnea frames in different EEG bands are shown in Fig. 2.5. Here, examples of both entropy and log-variance are presented for all the band limited signals. It is observed from the figure that the histograms of feature variation pattern corresponding to apnea and non-apnea cases differ widely from each other and the fitted Rician PDFs are different and have wide separation. Thus PDF model fitting is expected to offer better feature quality as well as reduced computational burden.

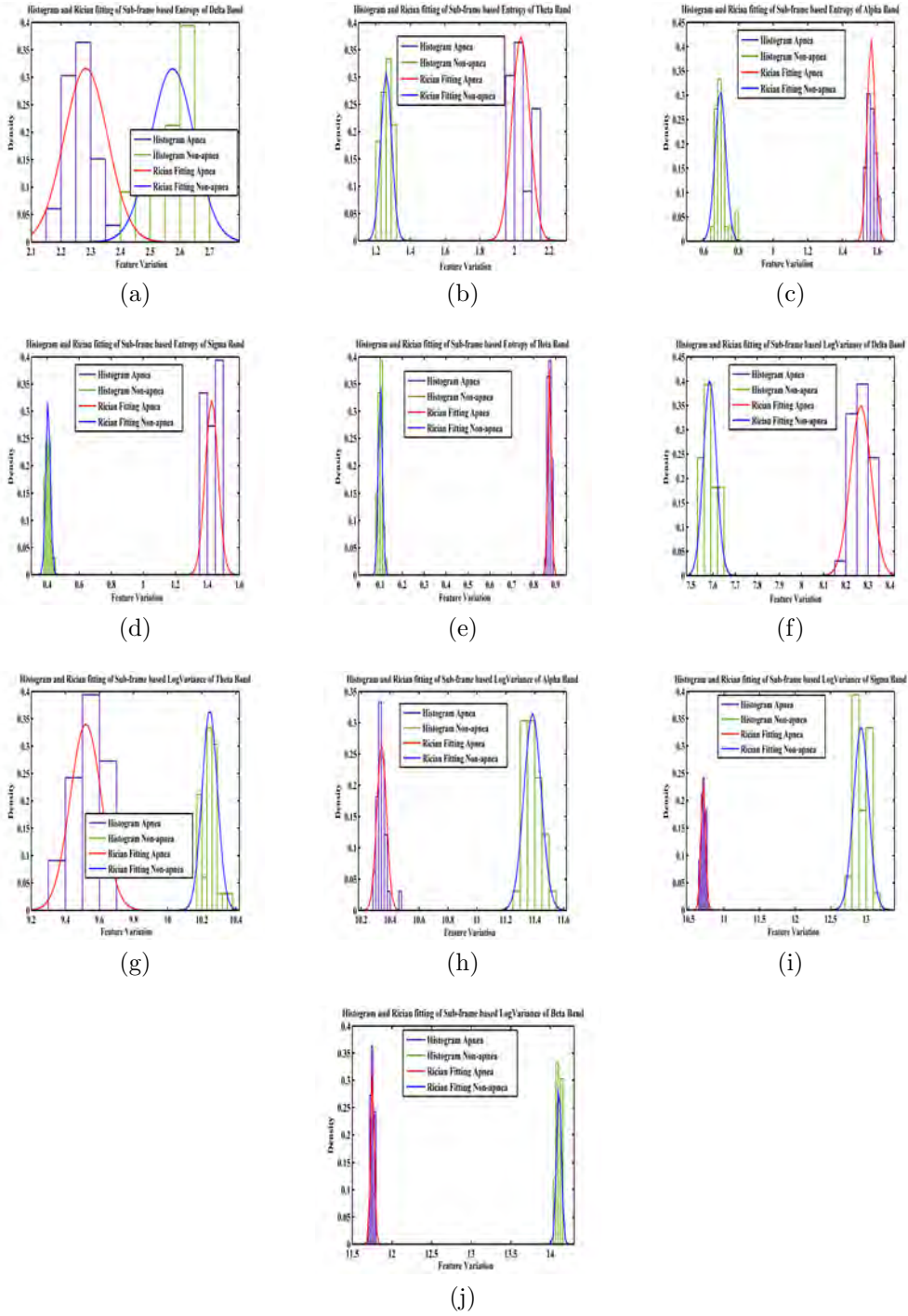


Figure 2.5: Histogram of Sub-frame based feature variation patterns of each sub-band and corresponding Rician fitting

Table 2.1: Definition of Characteristic PDFs

Distribution	PDF	Parameters
Normal	$f(x \mu, \sigma^2) = \frac{1}{\sigma\sqrt{(2\pi)}} \exp -\frac{(x-\mu)^2}{2\sigma^2}$	$\mu, \sigma$
Exponential	$f(x; \lambda) = \begin{cases} \lambda \exp^{-\lambda x}, & x \geq 0; \\ 0 & , x < 0 \end{cases}$	$\lambda$
Rayleigh	$f(x; \sigma) = \frac{x}{\sigma^2} \exp -\frac{x^2}{2\sigma^2}, x \geq 0$	$\sigma$
Rician	$f(x v, \sigma) = \frac{x}{\sigma^2} e^{-\frac{x^2+v^2}{2\sigma^2}} I_0(\frac{xv}{\sigma^2})$	$v, \sigma$
Gamma	$f(x; \alpha, \beta) = \frac{\beta^\alpha x^{\alpha-1} \exp^{-\beta x}}{\Gamma(\alpha)}$ ; $x > 0$ and $\alpha > 0 \beta > 0$	$\alpha, \beta$
Nakagami	$\frac{2m^m}{\Gamma(m)\Omega^m} x^{2m-1} \exp(-\frac{m}{\Omega} x^2)$ , $\forall x \geq 0; m \geq 0.5; \Omega > 0$	$m, \Omega$
Weibull	$f(x; \lambda, k) = \begin{cases} \frac{k}{\lambda} (\frac{x}{\lambda})^{k-1} \exp(-\frac{x}{\lambda})^k, & x \geq 0; \\ 0 & , x < 0 \end{cases}$	$\lambda, k$

For model parameter estimation Log-Likelihood method is adopted. The parameters which provide the maximum value of Log-Likelihood are taken as the estimated parameters. The statistical features and the model parameters calculated from each band limited signal of a frame are cascaded as stated in (2.3),(2.4) and (2.5) to form the final feature vector  $F_{\text{proposed}}$ . Here,  $F_{\text{stat},\delta}$  and  $F_{\text{mod},\delta}$  are the statistical features and model parameters, respectively extracted from both the sub-frame based entropy and log-variance feature variation patterns in delta band.  $F_{\text{statistical}}$  and  $F_{\text{model}}$  indicate the features obtained from statistical analysis

and model fitting, respectively.

$$\mathbf{F}_{statistical} = [\mathbf{F}_{stat,\delta} \ \mathbf{F}_{stat,\theta} \ \mathbf{F}_{stat,\alpha} \ \mathbf{F}_{stat,\sigma} \ \mathbf{F}_{stat,\beta}] \quad (2.3)$$

$$\mathbf{F}_{model} = [\mathbf{F}_{mod,\delta} \ \mathbf{F}_{mod,\theta} \ \mathbf{F}_{mod,\alpha} \ \mathbf{F}_{mod,\sigma} \ \mathbf{F}_{mod,\beta}] \quad (2.4)$$

$$\mathbf{F}_{proposed} = [\mathbf{F}_{statistical} \ \mathbf{F}_{model}] \quad (2.5)$$

### 2.1.5 Classifier

In the proposed method, K-nearest neighborhood (K-NN) classifier is used where distance function computed between the features belonging to the EEG pattern in the test set and K neighboring EEG patterns from both apnea and non-apnea group in the training set is considered. The test set EEG pattern is classified based on the K closer class labels of EEG patterns. For the purpose of performance evaluation, M-fold cross validation technique is employed.

## 2.2 Results and Discussions

The proposed method involves two stage feature extraction- features mentioned in Section 2.1.3 are computed from each sub-frame and the extracted feature variation pattern is used for statistical analysis and model fitting to obtain the final feature vector. In view of analyzing the performance of various models, different types of distributions are considered separately in forming the feature vector proposed in (2.4) and in particular Rician model is used in (2.5) to form the proposed feature vector. This Section presents description of the databases used and the detailed analysis on the choice of proper PDF, quality of the extracted features

and classification performance.

### 2.2.1 Database

In order to investigate the proposed method in discriminating apnea patients and healthy subjects as well as apnea and non- apnea frames of an apnea patient, the proposed method is evaluated on three large databases, publicly available in the PhysioNet [25] (Database-A), [26] (Database-B) and [27] (Database-C). Polysomnograms of healthy subjects are available in [27] while [25] and [26] contain full overnight polysomnograms from subjects with previously diagnosed with sleep apnea. Experienced sleep specialist scored the polysomnograms as apnea or non-apnea which is available as ground truth. Apnea and Hypopnea Index (AHI) defines the severity of apnea and it is measured by the number of occurrence per hour. For the purpose of detailed experimentation, subjects with broad variation in AHI are taken into consideration. In the databases there are different types of apnea and hypopnea, such as obstructive sleep apnea, central sleep apnea, mixed sleep apnea, obstructive sleep hypopnea, central sleep hypoapnea, and mixed sleep hypopnea. The proposed method is targeted to detect apnea frames irrespective of their types. All different categories of apnea and hypopnea events are termed as apnea in this work. Hence, all types of apnea and hypopnea frames and equivalent number of non-apnea frames for subjects with AHI greater than 5 are selected for experimentation. Depending on the available ground truth, for the databases available in [25] and [26], frame lengths are taken 15s and 30s, respectively. In terms of selecting sub-frame length ( $M$ ) and corresponding sample shift ( $p$ ), two factors are to be considered.

A small sub-frame length with a moderate sample shift will provide an increased number of feature variation data but it may result into incorrect estimation of the features due to not having enough data. Again, a very small sample shift can



be chosen which will provide a large number of feature variation data but it will increase computational complexity. Considering both the issues, in the proposed method, a relatively large sub-frame length of 1280 and 6250 samples are selected for databases- [25] and [26] and 90% overlap between two successive sub-frames are chosen to obtain better estimation of the features as well as considerable amount of data points for model fitting with moderate computational complexity. The information of the subjects used in this study and the number of EEG frames taken are given in Table 2.2.

### 2.2.2 Goodness of Model Fit

In this sub-section, a comparative analysis on fitting characteristics of different distributions is presented considering conventionally used statistical tools, such as Log Likelihood (LogL), Bayesian Information Criterion (BIC) and Akaike Information Criterion (AIC). The distribution with the largest Log Likelihood value represents statistically the best fit. BIC and AIC are defined as

$$BIC = -2 * \ln(\text{likelihood}) + [\ln(N)](k) \quad (2.6)$$

$$AIC = -2 * \ln(\text{likelihood}) + 2(k), \quad (2.7)$$

where  $N$  and  $k$  are the number of observations and degree of freedom of model, respectively. The best model in the group compared is the one that minimizes these scores.

In order to demonstrate the comparative fitting performance of various PDFs in multi-band sub-frame based feature variation patterns of each frame, above statistical parameters are calculated. The mean values of these statistical parameters

for all the apnea and the non-apnea frames corresponding to a subject are shown in Table 2.3. It is observed from the table the best PDF fitting performance is achieved by the Rician distribution and thus Rician distribution is used in the Proposed Method.

Table 2.3: Comparison of fitting of different distributions evaluated in Database-A

Distribution	Apnea			Non-apnea		
	LogL	BIC	AIC	LogL	BIC	AIC
Gamma	36.60	-66.21	-69.20	35.56	-64.12	-67.12
Weibull	35.89	-64.78	-67.78	34.51	-62.02	-65.02
Exponential	-60.95	125.39	123.89	-61.33	126.17	124.67
Rayleigh	-38.16	79.81	78.31	-38.54	80.58	79.09
<b>Rician</b>	<b>36.64</b>	<b>-66.29</b>	<b>-69.28</b>	<b>35.59</b>	<b>-64.18</b>	<b>-67.18</b>

The comparison of goodness of fit is also shown by probability plot in Fig. 2.6. Here, it is seen that Exponential, Rayleigh, Weibull do not show good fitting performances and it is also seen that Rician and Gamma are almost overlapped as they show similar performances. This also supports the values presented in Table 2.3.

### 2.2.3 Feature Quality Test

The quality of the proposed feature is investigated in terms of class separability by the standard goodness of feature measures, namely Bhattacharyya Distance (BD) and Geometrical Separability Index (GSI).

BD is a measure of similarity between two discrete or continuous probability distributions. It is closely related to the Bhattacharyya coefficient (BC) which is a measure of the amount of overlap between two statistical samples or populations. The BC can be used to determine the relative closeness of the two samples being considered. It is used to measure the separability of classes in classification. For



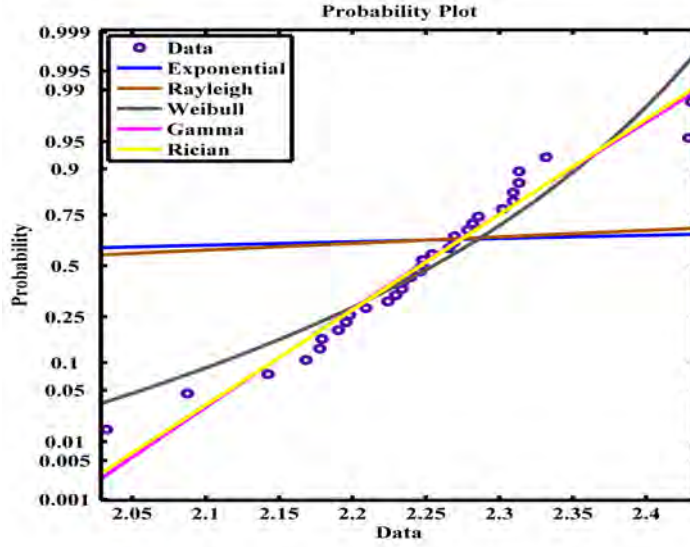


Figure 2.6: Probability Plot for fitting with different PDFs

two independent Gaussian data clusters, BD is computed as [28]

$$BD = \frac{1}{8}(\mu_2 - \mu_1)^T \left[ \frac{1}{2}(\delta_1 + \delta_2) \right]^{-1} (\mu_2 - \mu_1) + \frac{1}{2} \ln \left( \frac{\det(\frac{\delta_1 + \delta_2}{2})}{\sqrt{\det(\delta_1)} * \sqrt{\det(\delta_2)}} \right) \quad (2.8)$$

Here,  $\delta_i$  and  $\mu_i$  represent covariance matrix and mean vector of  $i$ -th cluster, respectively. Bhattacharyya coefficient (BC) is computed as

$$BC = \exp^{-BD} \quad (2.9)$$

Greater the value of Bhattacharyya distance, smaller the value of Bhattacharyya coefficient. Smaller value of Bhattacharyya coefficient represents smaller amount of overlap between two statistical samples or populations, thus ensures better feature quality.

GSI, called Thornton's separability index as well, gives the measure of the separability in the nearest neighbor sense of two classes. It is defined as the fraction of a set of data points whose labels for classification are similar to those

of their nearest neighbors. It is defined as [29]

$$GSI = \frac{\sum_{i=1}^N (f(x_i) + f(x'_i) + 1) \text{ mod } 2}{N} \quad (2.10)$$

where  $x'$  is the nearest neighbor of  $x$  and  $N$  denotes the number of points. Higher value of GSI and lower value of BC represent better the feature quality.

In Table 2.4 and 3.1, BC and GSI values are shown, respectively for subjects mentioned in Table 2.2 for database [25]. It can be observed from the table that out of several PDFs, the best feature quality, the lowest BC and the highest GSI is achieved by the Rician distribution and thus Rician distribution is selected to fit the sub-frame based feature sequence in the proposed method. Moreover, it is to be observed that the proposed feature combination of statistical analysis and Rician model parameters, as it is mentioned in (2.5) offers the best feature quality result.

For the data used in Table 2.2, box plots corresponding to Rician parameters ( $\nu, \sigma$ ) are shown in Fig. 2.7 where as distribution of statistical parameters are shown in Fig. 2.8. In both the cases, entropy variation of Beta band is considered. Here significant separation between the two classes (apnea and non-apnea) are observed.

## 2.2.4 Classification Result

For the purpose of classification, two different cases, (i) classification of apnea and non-apnea frames in the data of apnea patients and (ii) classification of apnea patients and healthy subjects, are considered. The K-NN classifier is used for classification. In classifier, various distance function and different value of  $K$  are tested. It is found that the cosine distance function and  $K=9$  give the best result.

Table 2.4: Feature Quality in terms of BC evaluated in Database-A

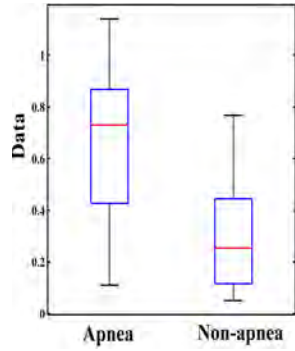
S/No.	Rayleigh	Exponential	Rician	Proposed
1	0.59	0.24	0.22	2.516E-06
2	0.43	0.44	0.37	2.05E-05
3	0.25	0.25	0.19	1.10E-05
4	0.33	0.43	0.31	5.78E-05
5	0.37	0.39	0.35	1.45E-05
6	0.57	0.48	0.33	3.22E-05
7	0.22	0.14	0.29	2.76E-06
8	0.09	0.06	0.04	1.71E-09
9	0.51	0.36	0.45	0.00036465
10	0.47	0.14	0.13	1.27E-06
11	0.11	0.12	0.33	6.04E-08
12	0.01	0.01	0.09	3.78E-10
13	2.57E-09	4.84E-10	2.43E-20	2.43E-24
14	0.07	0.07	0.21	3.12E-08
15	0.27	0.21	0.22	1.05E-05
16	0.25	0.20	0.11	1.88E-06
17	0.07	0.04	0.01	8.34E-22
18	0.59	0.48	0.48	0.00015511
19	0.20	0.27	0.29	7.32E-06
20	0.16	0.11	0.05	9.53E-09
21	0.38	0.15	0.10	4.05E-06
22	0.57	0.45	0.43	8.10E-05
23	0.59	0.50	0.38	6.96E-06
<b>Mean</b>	<b>0.31</b>	<b>0.24</b>	<b>0.23</b>	<b>3.36E-05</b>

Standard performance measures, namely sensitivity, specificity and accuracy, those are described in (2.11)-(2.13), and Table 2.6, are used.

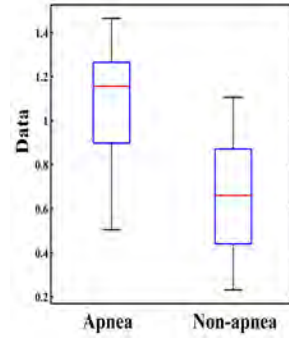
$$Accuracy(A_{cc}) = \frac{TP + TN}{TP + FP + TN + FN} * 100 \quad (2.11)$$

Table 2.5: Feature Quality in terms of GSI evaluated in Database-A

S/No.	Rayleigh	Exponential	Rician	Proposed
1	0.68	0.67	0.76	0.86
2	0.84	0.84	0.81	0.89
3	0.80	0.77	0.77	0.88
4	0.70	0.70	0.72	0.86
5	0.73	0.75	0.61	0.81
6	0.58	0.61	0.70	0.88
7	0.90	0.90	0.81	0.92
8	0.83	0.84	0.74	0.95
9	0.85	0.83	0.73	0.91
10	0.87	0.86	0.77	0.90
11	0.94	0.94	0.82	0.96
12	0.96	0.96	0.77	0.95
13	0.94	0.94	0.89	0.95
14	0.88	0.88	0.79	0.94
15	0.90	0.88	0.83	0.94
16	0.74	0.73	0.83	0.89
17	0.92	0.92	0.79	0.89
18	0.74	0.72	0.71	0.86
19	0.94	0.93	0.78	0.95
20	0.88	0.88	0.84	0.89
21	0.90	0.87	0.89	0.98
22	0.77	0.78	0.74	0.93
23	0.68	0.67	0.77	0.86
<b>Mean</b>	0.82	0.82	0.78	<b>0.91</b>

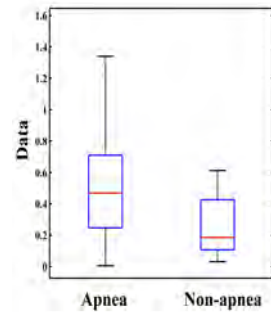


(a) Rician Model Parameter  $v$

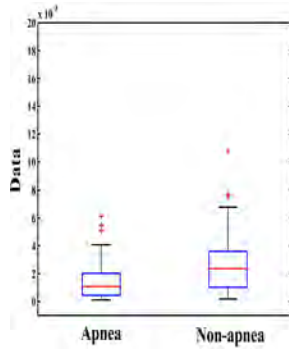


(b) Rician Model Parameter  $\sigma$

Figure 2.7: Box plot of model parameters



(a) Statistical Parameter  $\mu$



(b) Statistical Parameter  $\sigma$

Figure 2.8: Box plot of statistical parameters

$$Sensitivity(S_e) = \frac{TP}{TP + FN} * 100 \quad (2.12)$$

$$Specificity(S_p) = \frac{TN}{TN + FP} * 100 \quad (2.13)$$

Table 2.6: Definition of Accuracy Measures

	Apnea	Non-Apnea
Apnea	True Positive (TP)	False Negative (FN)
Non-apnea	False Positive (FP)	True Negative (TN)

### Classification of Apnea and Non-apnea Frames in the data of Apnea Patients

In this case, test and train, both data, are collected from the same subject.

**Effect of Use of Different PDFs** All three performance criteria obtained for each subject mentioned in Table 2.2 by using different PDFs are reported in Tables 4.1 and 4.2 for two databases using leave-one-out cross validation scheme. In these tables, ‘Stat’ represents a method that utilizes statistical features ( $F_{statistical}$ ) as described in Section 2.1.4. It is found that for both datasets, the specificity values obtained by using the proposed feature vector (Rician and statistical parameters) are comparable to those obtained by other methods. However, the sensitivity and accuracy values are found far superior to all other cases, which is the greatest

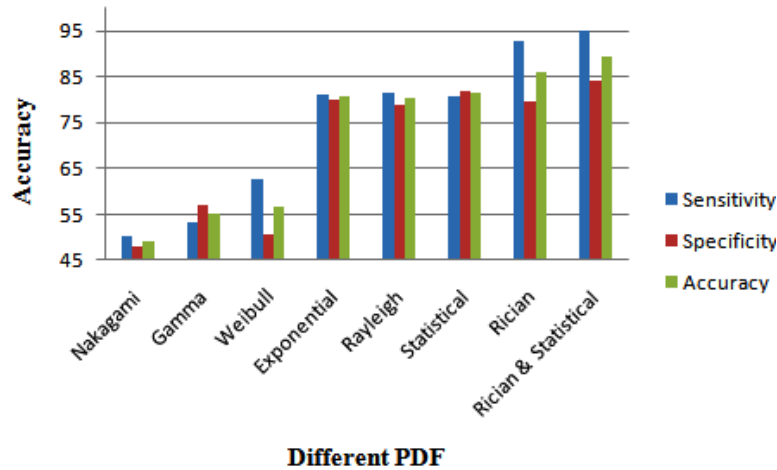


Figure 2.9: Performance criteria with different PDFs

Table 2.7: Classification result of leave-one-out cross validation evaluated in Database-A

S/No	Sensitivity(%)				Specificity(%)				Accuracy(%)						
	Exp.	Ray.	Stat.	Rician	Prop.	Exp.	Ray.	Stat.	Rician	Prop.	Exp.	Ray.	Stat.	Rician	Prop.
1	82.67	82.68	73.11	86.53	90.43	84.24	83.43	74.79	76.57	79.83	83.45	83.05	73.95	81.55	88.66
2	82.44	79.39	82.06	86.64	92.10	90.46	90.84	91.22	82.06	87.02	86.45	85.11	86.64	84.35	90.02
3	71.15	69.23	69.23	94.23	96.20	86.54	76.92	88.46	76.92	75.00	78.85	73.08	78.85	85.58	87.50
4	72.97	68.92	72.97	89.19	93.24	75.68	67.57	75.68	67.57	67.57	74.32	68.24	74.32	78.38	80.41
5	74.65	73.24	71.83	69.01	92.96	73.24	81.69	77.46	74.65	80.28	73.94	77.46	74.65	71.83	84.62
6	68.33	73.33	68.33	80.00	93.33	58.33	61.67	58.33	61.67	75.00	63.33	67.50	63.33	70.83	81.20
7	96.30	96.91	95.68	85.19	99.38	88.27	88.27	87.65	71.60	82.10	92.28	92.59	91.67	78.40	89.51
8	82.76	79.31	82.76	93.10	95.80	79.31	86.21	79.31	72.41	81.40	81.03	82.76	81.03	82.76	92.31
9	83.33	82.29	83.33	89.58	99.48	77.08	77.60	76.04	70.83	83.33	80.21	79.95	79.69	80.21	90.04
10	85.45	87.27	85.45	89.09	96.36	81.82	83.64	81.82	72.73	83.64	83.64	85.45	83.64	80.91	88.70
11	92.31	90.38	93.27	93.27	96.30	94.23	93.27	93.75	73.56	92.10	93.27	91.83	93.51	83.41	92.11
12	88.24	90.20	88.24	74.51	91.30	98.04	100.00	98.04	84.31	94.00	93.14	95.10	93.14	79.41	94.30
13	77.78	100.00	77.78	88.89	88.89	88.89	88.89	88.89	93.00	96.00	83.33	94.44	83.33	94.44	94.44
14	83.33	83.33	83.33	82.05	90.03	98.72	97.44	98.72	83.33	94.87	91.03	90.38	91.03	82.69	91.21
15	92.42	84.85	92.42	93.94	95.48	80.30	72.73	80.30	74.24	81.82	86.36	78.79	86.36	84.09	90.15
16	77.05	78.69	77.05	88.52	91.80	91.80	86.89	91.80	86.89	87.25	84.43	82.79	84.43	87.70	88.52
17	78.95	78.95	78.95	89.47	89.47	100.00	100.00	100.00	73.68	78.95	89.47	89.47	89.47	81.58	84.21
18	86.52	82.98	83.69	82.98	91.30	73.76	72.34	73.76	68.79	72.34	80.14	77.66	78.72	75.89	85.46
19	91.54	92.31	91.54	81.54	92.42	93.08	93.85	93.08	79.23	92.31	92.31	93.08	92.31	80.38	92.12
20	97.50	97.50	97.50	92.50	97.50	85.00	82.50	82.50	75.00	80.00	91.25	90.00	90.00	83.75	88.75
21	83.75	87.50	85.00	93.75	95.00	92.50	86.25	92.50	85.00	90.10	88.13	86.88	88.75	89.38	90.03
22	82.08	78.30	81.60	79.72	94.30	73.11	73.11	72.17	75.00	83.30	77.59	75.71	76.89	77.36	91.98
23	69.87	64.10	71.15	86.54	90.23	73.08	73.72	75.00	75.00	80.77	71.47	68.91	73.08	80.77	83.44
<b>Mean</b>	<b>82.67</b>	<b>82.68</b>	<b>82.42</b>	<b>86.53</b>	<b>93.77</b>	<b>84.24</b>	<b>83.43</b>	<b>84.39</b>	<b>76.25</b>	<b>83.60</b>	<b>83.45</b>	<b>83.05</b>	<b>83.40</b>	<b>81.55</b>	<b>88.68</b>

Table 2.8: Classification result of leave-one-out cross validation evaluated in Database-B

S/No	Sensitivity(%)						Specificity(%)						Accuracy(%)					
	Exp.	Ray.	Stat.	Rician	Prop.		Exp.	Ray.	Stat.	Rician	Prop.		Exp.	Ray.	Stat.	Rician	Prop.	
1	91.89	91.89	91.89	86.49	95.80		86.49	86.49	86.49	75.68	83.78		89.19	86.49	89.19	81.08	90.54	
2	80	80	80	92.31	87.69		83.08	76.92	83.08	73.85	81.54		81.54	76.92	81.54	83.08	84.62	
3	78.89	76.67	78.89	81.11	87.78		87.78	91.11	87.78	77.78	77.78		83.33	91.11	83.33	79.44	82.78	
4	73.81	66.67	73.81	71.43	78.57		92.86	95.24	92.86	69.05	84.20		83.33	95.24	83.33	70.24	83.33	
5	68.06	69.11	68.06	83.77	98.43		74.87	72.77	74.87	71.20	77.49		71.47	72.77	71.47	77.49	84.40	
6	84.35	83.48	83.48	85.65	97.39		72.61	72.17	72.61	72.61	80.43		78.48	72.17	78.04	79.13	88.91	
7	86.89	86.89	87.43	87.43	92.90		84.70	83.06	84.15	78.69	85.30		85.79	83.06	85.79	83.06	89.89	
8	92.91	88.65	92.91	97.87	98.58		68.09	70.21	68.09	73.76	74.47		80.50	70.21	80.50	85.82	86.52	
9	76	74	76	94	98		90	90	90	70	80		83	90	83	82	89	
10	100	98.53	100	100	100		89.71	91.18	89.71	89.71	89.71		94.85	91.18	94.85	94.85	94.85	
11	65.57	67.77	65.93	81.32	94.51		53.85	56.78	53.48	63.37	69.23		59.71	56.78	59.71	72.34	81.87	
12	87.14	87.14	87.14	91.43	91.43		84.29	87.14	84.29	87.14	90		85.71	87.14	85.71	89.29	90.71	
13	89	73	89	92	98		78	76	78	72	86		83.5	76	83.5	82	92	
14	84	84	84	100	100		74	74	74	82	82		79	74	79	91	91	
15	84	86	84	88	94		66	64	66	64	64		75	64	75	76	79	
<b>Mean</b>	<b>82.83</b>	<b>80.92</b>	<b>82.84</b>	<b>88.85</b>	<b>94.20</b>		<b>79.09</b>	<b>79.14</b>	<b>79.03</b>	<b>74.72</b>	<b>80.40</b>		<b>80.96</b>	<b>79.14</b>	<b>80.93</b>	<b>81.79</b>	<b>87.30</b>	



Table 2.9: Classification result of different cross-validation schemes evaluated in Database-A

Cross-validation	Sensitivity (%)					Specificity (%)					Accuracy (%)				
	Exp.	Ray.	Stat.	Rician	Prop.	Exp.	Ray.	Stat.	Rician	Prop.	Exp.	Ray.	Stat.	Rician	Prop.
leave-one-out	81.22	81.39	80.81	92.70	<b>93.77</b>	82.68	82.75	83.25	79.57	<b>83.60</b>	81.95	82.07	82.03	86.14	<b>88.68</b>
10-fold	83.82	85.55	82.85	91.39	<b>95.10</b>	79.57	81.79	83.20	76.05	<b>84.11</b>	81.80	83.19	83.02	83.00	<b>89.60</b>
5-fold	83.19	82.96	83.71	91.66	<b>92.27</b>	81.06	82.01	82.63	76.89	<b>80.93</b>	82.16	82.08	82.75	83.90	<b>87.56</b>
2-fold	82.88	81.97	83.43	90.27	<b>91.13</b>	80.55	79.87	79.47	71.12	<b>78.07</b>	81.65	80.40	81.21	80.13	<b>85.37</b>

advantage of the proposed scheme. For better understanding, the average of all three performance criteria for various PDFs is shown in Fig. 2.9. It is clearly observed from the figure that among different PDFs, Rician PDF offers the best sensitivity and accuracy, competitive specificity than that is obtained by other PDFs. At the same time, the proposed method gives the best result in terms of all three performance criteria. For the purpose of evaluating the consistency of the classification due to variation of amount of training data, results obtained by the proposed method by using the leave-one-out, 2-fold, 5-fold and 10-fold cross validation schemes are reported in Table 2.9. In all cases, similar to previous analyses, the best performance is obtained by the proposed scheme.

**Comparison of Proposed Method with Other Approaches** One major contribution of the proposed method is the use of two stage feature extraction: sub-frame based feature extraction and fitting the extracted feature variation using Rician PDF to use the model parameters as the feature. The proposed sub-frame based feature variation modeling is compared with the conventional frame based feature extraction method [16], [11], where features are calculated using the entire frame length. In the conventional approach, features (entropy and log-variance) are extracted from the entire band limited signals and directly used for classification. Instead of modeling the feature variation, another interesting comparison would be to consider the modeling of the data variation of the band limited sig-

Table 2.10: Comparison of the Proposed Method with Other Approaches

Measure	Database-A			Database-B		
	Data	Conventional	Prop.	Data	Conventional	Prop.
Sensitivity	73.21	81.03	<b>93.77</b>	71.06	81.96	<b>94.20</b>
Specificity	69.87	81.92	<b>83.60</b>	73.04	79.11	<b>80.40</b>
Accuracy	71.54	81.48	<b>88.68</b>	72.05	80.54	<b>87.30</b>
GSI	0.67	0.81	<b>0.91</b>	0.66	0.77	<b>0.87</b>

nals. The proposed method is compared with data modeling where the modeling and statistical analysis are carried out on the pre-processed band limited frame data. The comparison of the proposed method with the conventional approach and data modeling is presented in Table 2.10. It is evident from the table that proposed method offers significant improvement than the other two approaches in each performance criteria. Performance comparison is also carried out in terms of feature quality measure GSI. It is observed from the table that in terms of GSI, the proposed method offers superior feature quality compared to others. This is expected as the proposed sub-frame based feature extraction approach captures local feature information, which offers better local feature variation pattern than the other approaches.

The proposed method is also compared with some existing methods and results are reported in Table 2.11. In the implementation of the methods, for maintaining a fair comparison, frame length, sub-frame length, frequency limits for sub-bands, band pass filter, classifier parameters are kept same as the proposed method. It is observed from the table that the proposed method outperforms other methods significantly with respect to each performance criterion.

As an alternate, instead of analyzing proposed method individually for each subject, one may consider all frames from all the subjects mentioned in Table 2.2

and cross-validation schemes can be applied to evaluate the performance. The result obtained in this case is reported in Table 4.3. For each of 2-fold, 5-fold and 10-fold cross validation schemes ten independent trials are taken and average result is reported. It is clearly observable from the table that the proposed method offers very high sensitivity, good specificity and high accuracy in this case for all three evaluation schemes.

The proposed method detects all types of apnea and hypopnea as apnea. The sensitivity of the Proposed Method to different types of apnea and hypopnea are shown in Table 2.13. Here, it is evident that proposed method gives very satisfactory classification performances regardless of the type of apnea. The sensitivity of the proposed method is also investigated in terms of the severity of apnea, i.e. the AHI value of the subjects. It is known that AHI below 5 indicates healthy, from 5 to 15 is mild, above 15 to 30 is moderate and higher than 30 is severe [30]. The detailed result is given in Table 2.14. It is observed from the table that the method offers very high sensitivity irrespective of the high, low or medium AHI values.

The proposed method is also compared using different classification techniques as shown in Table 2.15. It is observed from the table that K-NN classifier gives

Table 2.11: Comparison of the Proposed Method with the Existing Methods

Method	Database-A			Database-B		
	Se.(%)	Sp.(%)	Acc.(%)	Se.(%)	Sp.(%)	Acc.(%)
[16]	77.69	79.96	78.83	72.143	66.46	69.302
[11]	65.74	59.15	62.45	60.30	56.50	58.40
[17]	81.47	83.28	82.38	80.084	80.647	80.366
[18]	72.40	70.31	71.36	71.62	69.88	70.75
[19]	78.4	76.3	77.35	76.62	74.88	75.75
<b>Proposed</b>	<b>93.77</b>	<b>83.60</b>	<b>88.68</b>	<b>94.20</b>	<b>80.40</b>	<b>87.30</b>

Table 2.12: Classification result with all subjects combined

Cross-Validation	Sensitivity (%)	Specificity (%)	Accuracy (%)
Leave-one-out	98.28	83.76	91.02
10-fold	95.86	82.90	89.37
5-fold	95.80	82.90	89.35
2-fold	94.96	80.70	87.83

Table 2.13: Sensitivity of the Proposed Method corresponding to Different Types of Apnea evaluated in Database-A

Types	Total Frames	Detected as Apnea	Sensitivity
Obstructive Apnea	323	321	99.38
Central Apnea	83	83	100
Mixed Apnea	51	51	100
<b>Total Apnea</b>	<b>457</b>	<b>455</b>	<b>99.56</b>
Obstructive Hypopnea	234	228	97.43
Central Hypopnea	277	270	97.47
Mixed Hypopnea	79	76	96.20
<b>Total Hypopnea</b>	<b>590</b>	<b>574</b>	<b>97.29</b>

the best performance, hence it is selected in the proposed method.

Average computational time is measured to extract features from one test signal where the whole process of computation is performed using Intel(R) Core(TM) i5-4200M processor with 2.50 GHz clock speed and 4 GB ram. It is found that for a test signal the proposed method takes about 72 ms which is very small and because of such small computation time, the proposed method can be applied for real time apnea detection.

### Classifying Apnea Patients and Healthy Subjects

Most of the methods available in literature deal with classification of EEG data collected from apnea patients and healthy persons. In this case, for the purpose

Table 2.14: Sensitivity of the Proposed Method Corresponding to Various AHI

Database-[25]		Database-[26]	
AHI	Sensitivity	AHI	Sensitivity
23	90.43	17	95.80
51	92.10	22.3	87.69
13	96.20	34	87.78
31	93.24	22.2	78.57
12	92.96	43	98.43
12	93.33	59.8	97.39
34	99.38	30.7	92.90
8	95.80	53.1	98.58
25	99.48	22.1	98
16	96.36	100.8	100
36	96.30	46.8	94.51
12	91.30	55.3	91.43
2	88.89	59.2	98
16	90.03	41.2	100
15	95.48	65.5	94
13	91.80		
7	89.47		
39	91.30		
24	92.42		
91	97.50		
14	95		
55	94.30		
46	90.23		

of testing, EEG signals corresponding to non-apnea events are generally collected from healthy subjects. On the contrary, it is always very challenging when frames of both classes come from a same subject, i.e., the task of discriminating apnea and non-apnea frames of an apnea patient which is already discussed in previous

Table 2.15: Performance Comparison Using Different Classifiers

Classifier	Sensitivity(%)	Specificity (%)	Accuracy (%)
SVM(Linear)	67	70	68.40
SVM (Polynomial)	87.32	91.28	89.30
SVM(RBF)	63.61	91.79	77.70
ANN	97.90	83.57	90.74
LDA	80.04	100	90.02
<b>K-NN</b>	<b>98.28</b>	<b>83.76</b>	<b>91.02</b>

Table 2.16: Classification result of Apnea and Healthy Data

Cross-Validation	Sensitivity (%)	Specificity (%)	Accuracy (%)
Leave-one-out	98.83	97.21	98.02
10-fold	98.68	96.51	97.61
5-fold	98.64	96.30	97.47
2-fold	98.33	96.24	97.28

subsection. In this sub-section, results on classifying apnea patients and healthy subjects are reported in Table 2.16. Healthy EEG data, used in this simulation are available in [27] and apnea frames of subjects of [25] mentioned in Table 2.2 are considered. In Table 2.16, leave-one-out, 2-fold, 5-fold, and 10-fold cross-validation results are reported. For each of the 2-fold, 5-fold and 10-fold cross validation schemes ten independent trials are considered and average result is reported. The result shows that the proposed method offers very satisfactory performances with respect to all the standard measures of performance criteria in classifying apnea and healthy EEG data.

## 2.3 Conclusion

In conventional frame-by-frame EEG data analysis only the global characteristics of a frame can be obtained as in that case, features are extracted considering the

entire frame at a time. On the contrary, in this work, two-stage feature extraction method is proposed. First, the feature is computed from small duration overlapping sub-frames within a frame, which can precisely capture sharp changes with respect to time and provide temporal variation of the extracted feature within that frame. Next, statistical analysis and modeling are carried out on the resulting feature variation pattern, which gives an opportunity to utilize both local and global characteristics of a frame. Apart from ensuring such time resolution in feature extraction, use of multi-band signals also ensures frequency resolution. Among various PDF models, it is found that the Rician PDF is offering the best feature quality in terms of Bhattacharyya distance and GSI. Irrespective of the type of apnea, the proposed method can not only classify apnea patient and healthy subject but also classify apnea and non-apnea frames of an apnea patient, which has a great demand in the overnight polysomnography (PSG) to reduce human error, labor and cost. The proposed method is evaluated on three different and large EEG databases and it offers superior classification performance in comparison to some existing methods in terms of sensitivity, specificity and accuracy. It makes the proposed method to be widely applicable in a greater domain of diagnosis.

## Chapter 3

# Model Based Apnea Detection Using Variational Mode Decomposed EEG Signal

In this Chapter, instead of using multiple bio-signals, an automatic sleep apnea detection scheme is proposed using single lead EEG signal, which is computationally efficient and cost effective. Here, both classification scenarios- classifying apnea and non-apnea frames in the data of an apnea patient and classification of apnea and healthy subjects, are taken into consideration. The given raw EEG frame is pre-processed and divided into overlapping sub-frames. Variational mode decomposition (VMD) analysis is introduced in each sub-frame and features are extracted from each mode. VMD gives an opportunity to obtain compact BLIMFs with adaptive center frequencies in direct relevance to the varying neural activity of brain. Instead of directly using the extracted feature vector, within frame feature value variation pattern is modeled with a suitable characteristic probability distribution function (PDF) and the fitted model parameters are then used in K nearest neighbor (K-NN) classifier to classify apnea and non-apnea frames.



Extensive experimentation is carried out on the same dataset used in previous Chapter.

### 3.1 Proposed Method

Features are extracted from the mode functions obtained from each sub-frame by applying VMD and finally temporal variation of each feature is modeled with a suitable PDF. Different major steps involved in the proposed method is presented in Fig. 3.1. Detailed description of the steps is presented in this Section.

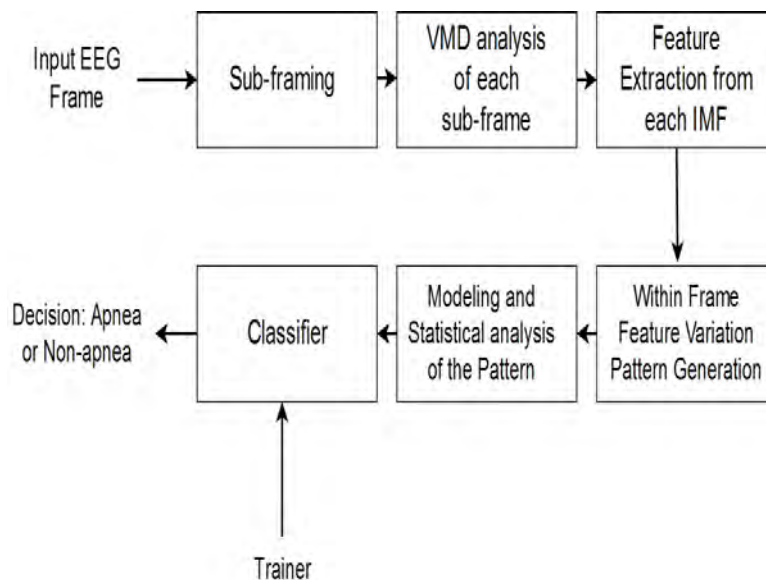


Figure 3.1: Flow chart of the Proposed method

#### 3.1.1 Analysis with Sub-framing

DC offset removal and frame amplitude normalization is performed in each frame for pre-processing. Neural activity level of the recorded EEG signal changes with respect to time during sleep. Hence, in different EEG frames, there exists a large variation in energy content. To counter this phenomena, in each frame, energy

normalization is also applied. Usually, in frame by frame analysis, the analysis of a test frame is carried on the full duration. In this work, as an alternate, sub-frame based analysis is proposed where the test frame is divided into a shorter frame duration (to be called sub-frame) and reasonable amount of time overlap is kept between successive sub-frames to obtain several sub-frames.

Sub-framing operation is carried out as like [15]. For example, from frame of  $N$  length, with sub-frame duration of  $M$  samples and shifting it by  $p$  samples, the second sub-frame can be found from  $(p + 1)th$  sample to  $(p + M)th$  sample. This procedure can be continued till reaching the end of the frame. Considering  $p \ll M < N$ , total  $\frac{N-M}{p} + 1$  sub-frames can be obtained.

### 3.1.2 Short Description of Variational Mode Decomposition (VMD)

The VMD algorithm decomposes any input signal adaptively into  $k$  discrete number of band-limited intrinsic mode functions ( $u_k$ ). Here each mode is mostly compact around the respective center frequency  $\omega_k$ . The algorithm searches for a given number of  $u_k$  and the corresponding center frequencies  $\omega_k$  utilizing alternate direction method of multipliers (ADMM). Input signal can be reproduced either exactly or in least square sense by using these modes. Detailed description of VMD algorithm can be found in [31]. The major steps involved in the VMD algorithm can be briefly summarized as-

- i) for each mode  $u_k$ , the associated analytic signal is computed using Hilbert transform in order to obtain a unilateral frequency spectrum
- ii) Mode's frequency spectrum is shifted by mixing with an exponential tuned to the respective calculated center frequency
- iii) Bandwidth is estimated through Gaussian smoothness of the demodulated signal

To search for  $u_k$  and  $\omega_k$ , it is required to solve a constrained variational problem, which is described by the following equation:

$$\left( \begin{array}{c} \min \\ u_k, \omega_k \end{array} \right) = \left\{ \sum_k \left\| \partial_t \left[ \left( \delta(t) + \frac{j}{\pi t} \right) * u_k(t) \right] e^{-j\omega_k t} \right\|_2 \right\}, \quad (3.1)$$

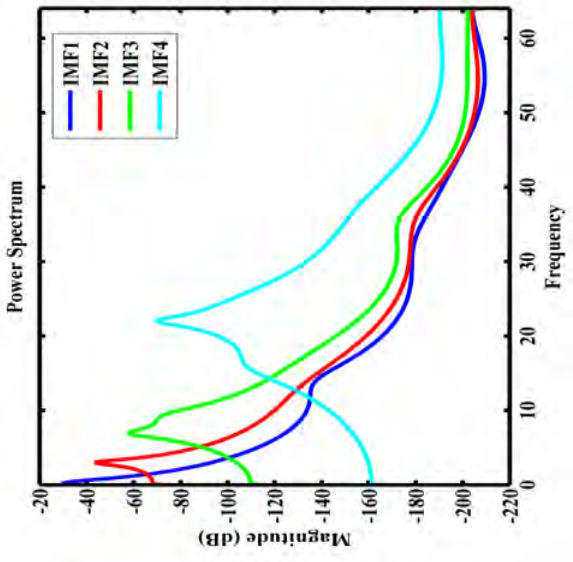
$$\sum_k u_k = f \quad (3.2)$$

where  $t$  is the time script,  $\delta(\cdot)$  is the Dirac distribution and  $*$  denotes convolution operator,  $f$  is the signal to be decomposed and  $k$  is the number of modes.

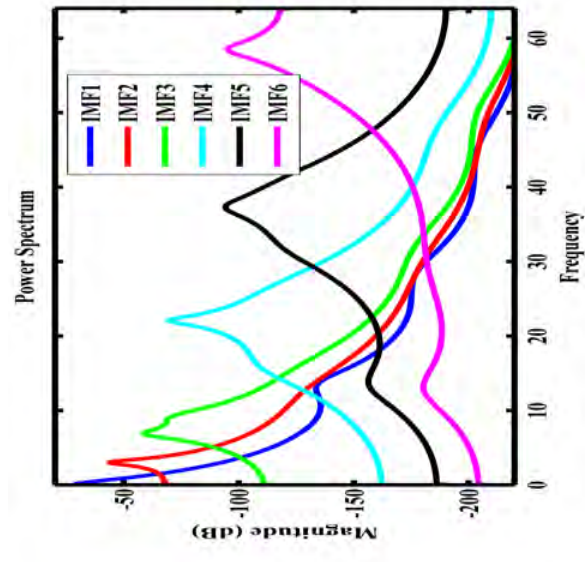
The number of modes has to be predefined in the application of VMD and its value (underbinning or overbinning) has considerable impact on the quality of decomposed signals. In different applications, EEG signal is divided into five frequency band-limited signals, namely- delta (0.25-4 Hz), theta (4-8 Hz), alpha (8-12 Hz), sigma (12-16 Hz) and beta (16-40 Hz), where the frequency bands are well established in literature and exhibit differences in frequency (Hz), amplitude and activity level. Delta, theta and alpha bands correspond to deep sleep, mild sleep and relax state, respectively while sigma and beta bands refer to alert states [32]-[33]. During apnea, as the breathing is paused, level of carbon dioxide rises in the bloodstream. Increased carbon dioxide level in the bloodstream is recognized by the chemoreceptors. As a result, person sleeping is signaled by brain to breathe in air and wake up [23]. Hence, there can be significant variation in different EEG frequency bands due to the above mentioned changes in neural activity from non-apnea to apnea. However, in a particular band, it is expected that the dominant frequencies caused by neural activity shift slightly from time to time and person to person.

Hence, simple bandpass filtering of EEG data with fixed center frequency will not be able to capture the shifts. VMD analysis results in band limited IMFs where

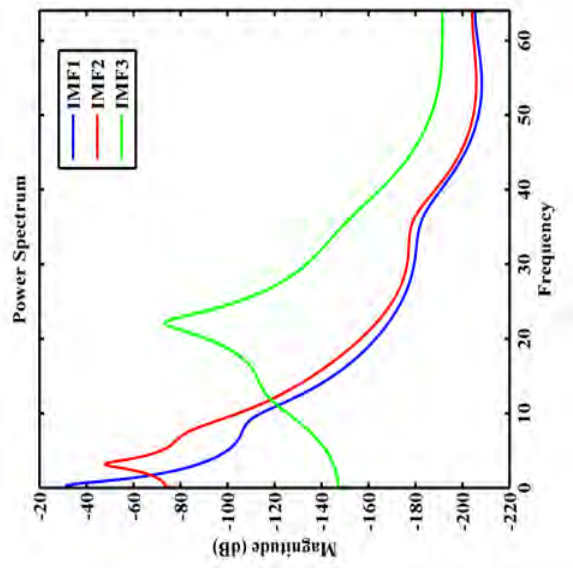
the center frequencies are dynamically calculated. This allows center frequency to shift and accurately represent the neural activity. Moreover, in order to correspond with the variation of neural activity in different frequency bands, the number of VMD modes should be chosen in such a way that both lower and higher frequency bands are covered. In order to present variation in spectral representation for various number of modes, in Fig. 3.2, a frame of EEG data is considered and power spectral densities are plotted for different number of VMD modes. It is observed that  $K=3$  and 4 do not have modes covering frequency above 30 Hz. Moreover,  $K=4$  has mode at around 10 Hz, representing original alpha state, which is missing for  $K=3$ . For  $K=5$  the earlier four modes stay on their positions and an extra mode appears covering higher frequency band ( $>40$  Hz). Higher frequency band is further divided into increased number of modes as the value of  $K$  is taken greater than five. As EEG data mostly have significant information lying in lower bands (frequency  $<40$  Hz), it is redundant to have too many modes in higher frequency. Division of higher frequency band into more bands corresponding to new modes does not provide necessary information for apnea detection. Moreover, increase of number of modes increases computational complexity. Hence, in this work  $k=5$  is proposed to utilize the entire frequency band and to have modes representing conventional EEG Sub-bands. Moreover, it also ensures of not having redundant modes increasing the computational complexity. Detailed performance comparison with various number of modes is given in Section 3.2.



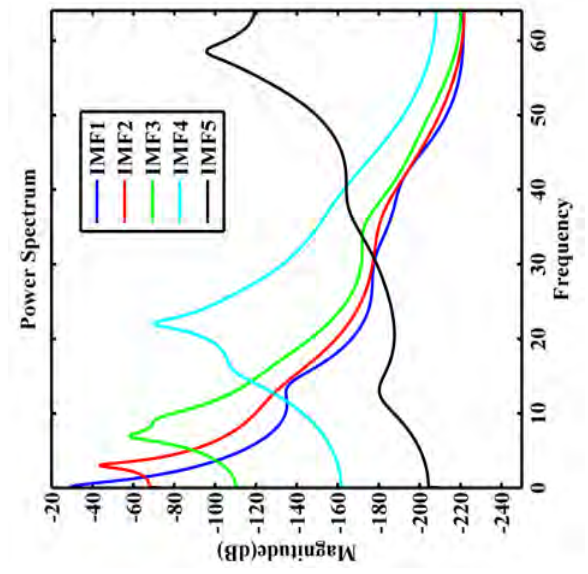
(a)



(b)



(c)



(d)

Figure 3.2: Power spectrum densities of  $K$  number of VMD modes of an EEG frame (a)  $K=3$  (b)  $K=4$  (c)  $K=5$  (d)  $K=6$

The frequency characteristics can be further presented by demonstrating the variation of center frequencies of each IMF of the sub-frames within a frame for both apnea and non-apnea. The frequency signature is presented in Fig. 3.3. Here for each sub-frame center frequencies are calculated and plotted for each IMF. As it is mentioned above that different VMD IMFs represent different frequency bands, which is clearly visible from the figure.

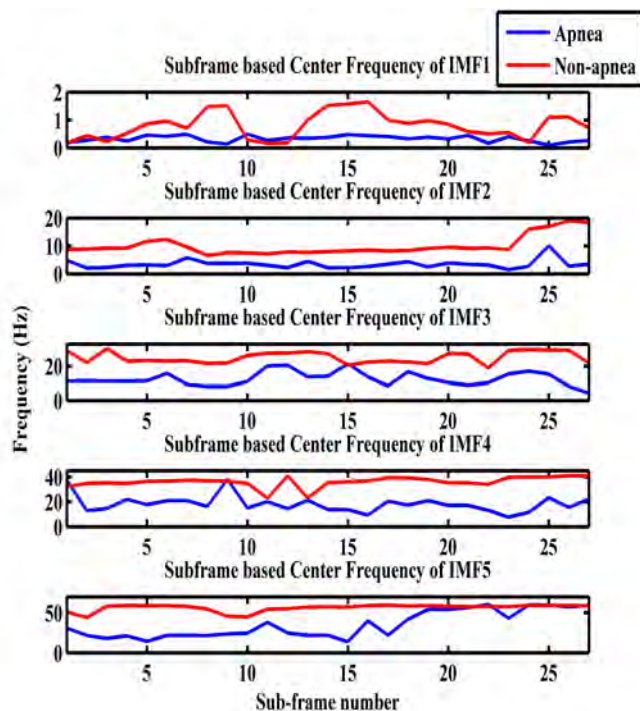


Figure 3.3: Frequency Signature of the Proposed method

### 3.1.3 Proposed Features for each mode

During apnea, patients experience disturbance in normal breathing and this can lead to grunting, gasping, body movements. Hence, it is expected that there will be changes in information content in EEG signal during apnea events as EEG corresponds directly with various neural activity level. Moreover, variation in

EEG data increases during apnea than non-apnea instances. Such changes in information content and the data variation are expected to be better reflected in different VMD modes of sub-frame EEG data than whole duration frame. In order to capture the changes, in the proposed method, entropy and log-variance are chosen as features to be extracted from each VMD mode of sub-frame EEG data. Detailed calculation of the features are mentioned in Section 2.1.2 of the Chapter.

### 3.1.4 Feature Variation Pattern Generation

In the proposed sub-frame based VMD analysis scheme, features are extracted from each mode of overlapping sub-frames. If the amount of frame shifting ( $p$ ) in sub-framing is kept small, features extracted for each mode in sub-frame based VMD analysis can provide a precise variation profile of that feature characteristic. Such use of sub-frame and VMD provides an opportunity to obtain a temporal variation profile of a particular feature for a specific mode within a frame. If there are  $W$  number of sub-frames, the within frame feature variation pattern for  $k$ th mode can be generated as

$$\textit{Variation Pattern} = [F_{1k}, F_{2k}, F_{3k}, \dots, F_{Wk}], \quad (3.3)$$

where  $F_{Wk}$  denotes the feature calculated from the  $k$ th mode of the  $W$ th sub-frame.

In order to represent the within frame feature variation in different VMD modes, in Fig. 3.4, entropy values calculated from different modes are presented for both apnea and non-apnea. Entropy values are calculated in proposed sub-frame based VMD analysis from each modes and the variation patterns of entropy values are shown. It is evident that in different modes, characteristics of feature variation is different from apnea to non-apnea.

### 3.1.5 Processing of the Extracted Feature Sequence

Within frame feature variation pattern can be directly given as input to classifier. But sub-framing calculates more number of features for a single frame than compared to conventional feature extraction method. Hence, if sub-frame based extracted features are directly utilized for classification, it will increase the feature dimension considerably, which will in a way affect the computational time and cost. As an alternate, characteristics of feature variation profile can be investigated for classifying apnea and non-apnea frames. One idea can be to carry out statistical analysis on feature variation pattern. Among various statistical features, in the proposed method, mean and variance are used.

Furthermore, amplitude variation of the feature variation pattern of each VMD mode can be investigated. In this paper, we propose to fit the sub-frame based feature variation pattern with probability density function (PDF). The motivation is to use the parameters of the fitted PDF as feature. In the choice of different PDFs, well known PDFs can be considered. Such approach can investigate the data distributions of feature variation profile. As model parameters are mostly one or two, problem regarding large feature dimension is eliminated and the computational burden is reduced. Among different PDFs, in this work, we propose to fit the feature variation pattern with Rician PDF.

Detailed analyses with different PDFs are covered in Section 3.2. Histograms of feature variation patterns and the corresponding Rician fittings of various apnea and non-apnea frames for different VMD modes are presented in Fig. 4.4. It is evident from the figure that the fitted Rician PDFs for apnea and non-apnea frames differ widely and there are minimum overlap between the two. Hence the fitted parameters are expected to quantify the variation pattern better and to have better feature quality.



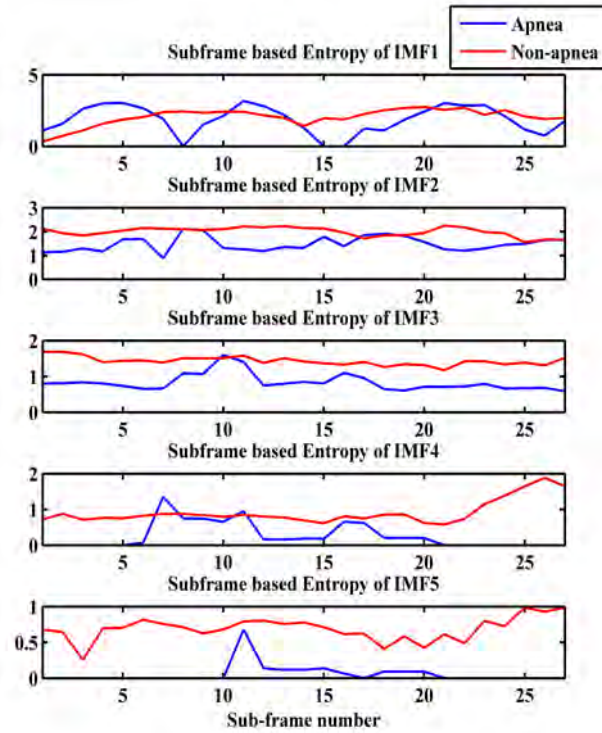


Figure 3.4: Entropy feature variation obtained from different IMFs of VMD of both apnea and non-apnea. Here, test frame is divided into multiple sub-frames and each sub-frame is variational mode decomposed. Entropy is calculated from each resulting IMF and the variation profile of with-in frame entropy feature is plotted.

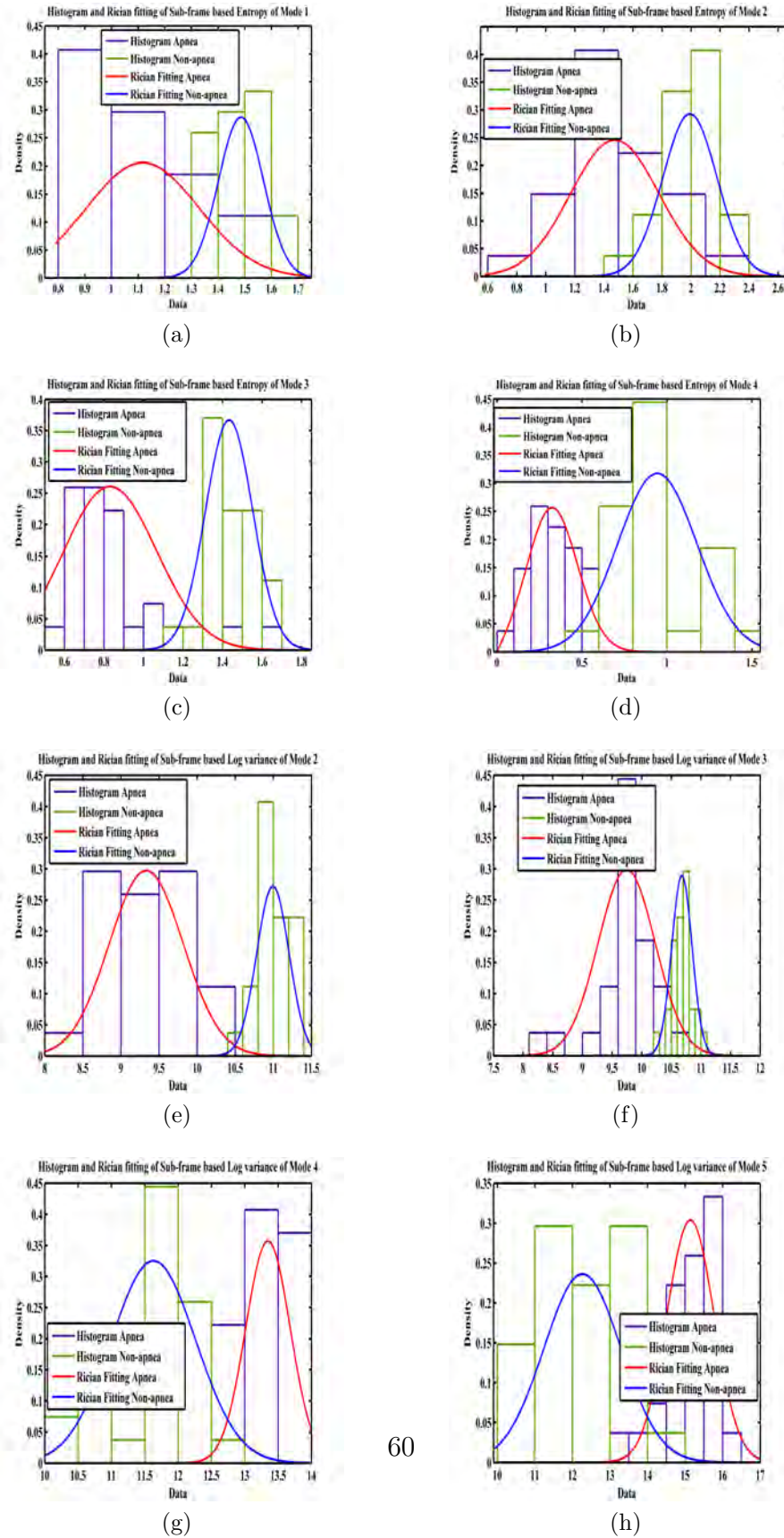


Figure 3.5: Histograms of the calculated feature variation patterns and the corresponding Rician fittings of various VMD modes for both apnea and non-apnea frames.

The statistical features ( $F_{\text{statistical}}$ ) and the model parameters ( $F_{\text{model}}$ ) calculated from each mode of overlapping sub-frames of a frame are cascaded as equation (3.4),(3.5) and (3.6) to obtain the final feature vector ( $F$ ). Here,  $F_{\text{mod},1}$  and  $F_{\text{stat},1}$  are the model parameters and statistical features, respectively, calculated from the feature variation patterns of mode 1.

$$\mathbf{F}_{\text{statistical}} = [\mathbf{F}_{\text{stat},1} \ \mathbf{F}_{\text{stat},2} \ \dots \ \mathbf{F}_{\text{stat},n}] \quad (3.4)$$

$$\mathbf{F}_{\text{model}} = [\mathbf{F}_{\text{mod},1} \ \mathbf{F}_{\text{mod},2} \ \dots \ \mathbf{F}_{\text{mod},n}] \quad (3.5)$$

$$\mathbf{F} = [\mathbf{F}_{\text{statistical}} \ \mathbf{F}_{\text{model}}] \quad (3.6)$$

## 3.2 Results and Discussions

In the proposed method, a frame of EEG data is preprocessed and divided into overlapping sub-frames. VMD analysis is performed on each sub-frame signal. Features mentioned in Section 3.1.3, are calculated for each mode. The feature variation patterns obtained for each mode are subjected to model fitting and statistical analysis and the final feature vector is formed according to (3.4),(3.5) and (3.6). In the following Sections the database description, feature quality analysis and the classification results of sleep apnea detection are presented.

### 3.2.1 Database

For the purpose of experimentation, subjects mentioned in Table 2.2 in Chapter 2 are used in this work. For [25] and [26], frame durations taken are 15s and 30s, respectively, depending on the respective ground truths. There are two consid-

erations to make in selection of sub-frame duration and the size of overlap. A big sub-frame length with large overlap will not provide enough data for feature variation pattern and thus the corresponding model fitting will be biased. On the other hand, a very small sub-frame length with large overlap is an option but very short sub-frame length might provide incorrect estimate of features, such as entropy and log-variance. Moreover, large overlap between consecutive sub-frames will result into a large number of feature variation data that will increase the computational complexity. Hence, keeping both the issues in consideration, in this work a moderate sub-frame length of 2s and 4s are used for databases- [25] and [26], respectively and 80% overlap between two successive sub-frames are maintained to ensure enough data points for model fitting with moderate computational complexity.

### 3.2.2 Feature Quality Test

Quality of the proposed feature vector is analyzed by the goodness of feature measures such as, Geometrical Separability Index (GSI). GSI, called Thornton's separability index as well, gives the measure of the separability in the nearest neighbor sense of two classes. It is defined as the fraction of a set of data points whose labels for classification are similar to those of their nearest neighbors. It is defined as [29]

$$s = \frac{\sum_{i=1}^N (f(x_i) + f(x'_i) + 1) \text{ mod } 2}{N}, \quad (3.7)$$

where N is the number of data points and  $x'$  is the nearest neighbor of  $x$ .

From (3.7) it is understandable that separability index,  $s$  approximates to one when two classes are separable and zero for inseparable classes, hence higher the GSI value, better the feature quality. In Table 3.1, GSI values are given for the

purpose of comparison among method of different distribution fitting to multi-band feature variation pattern and the proposed method. From Table 3.1 it is evident that out of different PDFs, Rician PDF fitting gives better performance, while the proposed method of combining Rician PDF parameter and statistical features, offers the best GSI index.

The distribution of Rician parameters ( $\nu$ ,  $\sigma$ ) are presented in Fig. 3.6 via boxplot using the data of Table 2.2. Here entropy feature variation in mode 5 is considered. It is obvious from the figure that there is are significant separation in distribution of the parameters between apnea and non-apnea.

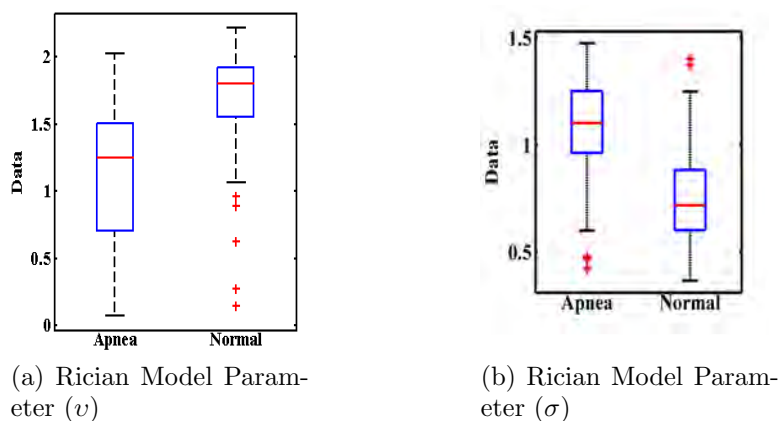


Figure 3.6: Distribution of model parameters

### 3.2.3 Classification Result

As like Chapter 2, for classification purpose, in this work, two distinct cases are considered, (i) apnea and non-apnea classification in the data of apnea patients and (ii) apnea patients and healthy subjects classification. In K-NN classifier, cosine distance function and  $K$  equal to 9 are chosen. Standard performance measures described in (2.11)-(2.13) are used to evaluate the performance of the proposed method. These were computed using TP, FP, FN, and TN values [34] as shown in

Table 3.1: Feature Quality by GSI evaluated in Database-A

S/No.	Gamma	Ray.	Exp.	Stat.	Rician	Proposed
1	0.71	0.84	0.84	0.84	0.81	0.92
2	0.73	0.93	0.92	0.96	0.84	0.99
3	0.63	0.76	0.75	0.79	0.66	0.85
4	0.49	0.64	0.65	0.64	0.58	0.75
5	0.73	0.72	0.70	0.70	0.75	0.75
6	0.63	0.86	0.83	0.79	0.69	0.87
7	0.78	0.80	0.80	0.92	0.93	0.94
8	0.84	0.78	0.76	0.88	0.86	0.95
9	0.79	0.87	0.86	0.89	0.84	0.95
10	0.66	0.76	0.73	0.69	0.72	0.83
11	0.80	0.91	0.89	0.92	0.84	0.93
12	0.78	0.94	0.94	0.97	0.94	0.99
13	0.76	0.83	0.83	0.89	0.72	0.94
14	0.82	0.95	0.93	0.93	0.95	0.97
15	0.64	0.85	0.84	0.84	0.86	0.92
16	0.66	0.84	0.81	0.90	0.77	0.95
17	0.77	0.84	0.82	0.84	0.87	0.92
18	0.63	0.68	0.69	0.67	0.74	0.88
19	0.72	0.83	0.82	0.89	0.89	0.95
20	0.76	0.93	0.93	0.90	0.86	0.91
21	0.72	0.83	0.81	0.92	0.85	0.98
22	0.67	0.71	0.68	0.73	0.87	0.89
23	0.69	0.78	0.76	0.81	0.81	0.92
<b>Mean</b>	0.71	0.82	0.81	0.84	0.81	<b>0.91</b>

Table 2.6.

### **Classification of Apnea and Non-apnea Frames in the data of Apnea Patients**

Here, only apnea patients are considered, where test and train data are from the same patient. Healthy subjects are not considered here.

**Performance Analysis of Different PDFs** For every subject mentioned in Table 2.2 the proposed method is evaluated for different PDFs. Performance analyses using leave-one-out cross validation technique for each PDF are reported in Tables 3.2 and 3.3 for databases [25] and [26], respectively .

In the tables, ‘Stat’ represents the method utilizing statistical features ( $F_{statistical}$ ) as mentioned in (3.4). From the results reported in Tables 3.2 and 3.3, it is found that for both the datasets, specificity values acquired by the proposed feature set (Rician parameters and statistical analyses) are similar to those achieved by other PDFs. But, the sensitivity and the accuracy values are found to be far better compared to all other cases. Greater sensitivity means high apnea detection performance, hence it serves as a big advantage of the proposed method. The mean of the performance criteria for different PDFs is presented in Fig. 3.7. As found earlier, among different PDFs, Rician PDF offers the best sensitivity and accuracy and competitive specificity whereas, the proposed method achieves the best performance in each criteria.

**Comparison of Proposed Method with Other Approaches** Comparison of the proposed sub-frame based analysis is carried out with the conventional feature extraction method. In the conventional approach, instead of using sun-framing, the features are computed using the entire frame duration and directly used as

Table 3.2: Performance analysis of the proposed method for various PDF fitting using leave-one-out cross validation (database-A)

S/No.	Sensitivity(%)			Specificity(%)			Accuracy(%)								
	Exp.	Ray.	Stat.	Rician	Prop.	Exp.	Ray.	Stat.	Rician	Prop.	Exp.	Ray.	Stat.	Rician	Prop.
1	86	86	88	98	92	92	90	86	82	90	89	88	87	90	91
2	92.62	94.67	94.67	97.13	98.36	93.44	96.72	96.72	80.33	96.72	93.03	95.70	95.70	88.73	97.54
3	82	82	88	74	90	80	80	88	68	86	81	81	88	71	88
4	62.16	58.11	58.11	58.11	77.03	78.38	75.68	81.08	71.62	71.62	70.27	66.89	69.59	64.86	74.32
5	71.83	73.24	76.06	77.46	83.10	80.28	80.28	77.46	76.06	81.69	76.06	76.76	76.76	76.76	82.39
6	76.60	78.72	72.34	95.74	100	82.98	82.98	78.72	65.96	87.23	79.79	80.85	75.53	80.85	93.62
7	70.08	69.29	85.83	98.43	96.06	93.70	96.06	92.13	89.76	91.34	81.89	82.68	88.98	94.09	93.70
8	75.86	68.97	68.97	93.10	82.76	79.31	86.21	86.21	82.76	86.21	77.59	77.59	77.59	87.93	84.48
9	92.55	92.02	90.96	92.55	98.40	84.04	86.17	86.70	80.85	88.30	88.30	89.10	88.83	86.70	93.35
10	76.36	76.36	81.82	87.27	90.91	83.64	83.64	74.55	61.82	85.45	80	80	78.18	74.55	88.18
11	87.98	89.90	87.50	97.12	98.56	87.98	87.98	89.42	79.81	87.02	87.98	88.94	88.46	88.46	92.79
12	94.12	94.12	94.12	94.12	96.08	100	100	100	100	100	97.06	97.06	97.06	97.06	98.04
13	88.89	88.89	88.89	88.89	88.89	100	100	88.89	100	100	94.44	94.44	88.89	94.44	94.44
14	97.44	97.44	91.03	100	94.87	93.59	94.87	97.44	92.31	97.44	95.51	96.15	94.23	96.15	96.15
15	91.80	93.44	91.80	96.72	98.36	81.97	78.69	83.61	77.05	73.77	86.89	86.07	87.70	86.89	86.07
16	84.21	87.72	92.98	92.98	98.25	94.74	94.74	89.47	78.95	89.47	89.47	91.23	91.23	85.96	93.86
17	94.74	89.47	89.47	100	100	73.68	73.68	68.42	73.68	73.68	84.21	81.58	78.95	86.84	86.84
18	75.71	75	74.29	93.57	97.14	67.14	68.57	71.43	65	72.14	71.43	71.79	72.86	79.29	84.64
19	93.75	92.86	91.07	94.64	96.43	86.61	86.61	88.39	92.86	92.86	90.18	89.73	89.73	93.75	94.64
20	95	97.5	95	95	97.50	85	85	87.50	82.50	80	90	91.25	91.25	88.75	88.75
21	80	75.38	89.23	98.46	92.31	92.31	95.38	93.85	84.62	96.92	86.15	85.38	91.54	91.54	94.62
22	80.19	81.13	81.60	94.81	97.64	66.51	66.51	72.17	80.66	81.60	73.35	73.82	76.89	87.74	89.62
23	81.41	83.33	84.62	89.74	97.44	82.69	83.33	85.90	74.36	89.74	82.05	83.33	85.26	82.05	93.59
<b>Mean</b>	83.97	83.72	85.06	91.65	<b>94</b>	85.22	85.79	85.39	80.04	<b>86.92</b>	84.59	84.75	85.23	85.84	<b>90.46</b>



Table 3.3: Performance analysis of the proposed method for various PDF fitting using leave-one-out cross validation (database-B)

S/No.	Sensitivity(%)						Specificity(%)						Accuracy(%)								
	Exp.	Ray.	Stat.	Rician	Prop.	Exp.	Ray.	Stat.	Rician	Prop.	Exp.	Ray.	Stat.	Rician	Prop.	Exp.	Ray.	Stat.	Rician	Prop.	
1	85.71	82.86	91.43	88.57	94.29	88.57	88.57	97.14	94.29	94.29	87.14	85.71	94.29	91.43	94.29	87.14	85.71	94.29	91.43	94.29	94.29
2	81.54	83.08	84.62	90.77	95.38	86.15	87.69	83.08	69.23	83.08	83.85	85.38	83.85	80	83.85	83.85	85.38	83.85	80	83.85	89.23
3	76.67	77.78	82.22	83.33	90.00	88.89	88.89	88.89	73.33	83.33	82.78	83.33	83.33	78.33	83.33	82.78	83.33	85.56	78.33	83.33	86.67
4	80.95	80.95	69.05	78.57	78.57	83.33	85.71	90.48	69.05	76.19	82.14	83.33	79.76	73.81	76.19	82.14	83.33	79.76	73.81	76.19	77.38
5	75.39	74.87	70.16	81.68	97.38	73.82	74.35	78.53	73.30	76.96	74.61	74.61	74.35	77.49	76.96	74.61	74.61	74.35	77.49	76.96	87.17
6	95.65	95.65	93.04	78.26	100	73.48	74.78	77.39	66.52	85.22	84.57	85.22	85.22	72.39	85.22	84.57	85.22	85.22	72.39	85.22	92.61
7	78.69	75.41	86.34	87.43	96.72	77.05	81.97	85.25	74.86	90.16	77.87	78.69	85.79	81.15	90.16	77.87	78.69	85.79	81.15	90.16	93.44
8	83.21	82.44	80.15	89.31	96.18	78.63	80.15	68.70	71.76	76.34	80.92	81.30	74.43	80.53	76.34	80.92	81.30	74.43	80.53	76.34	86.26
9	88	88	82	94	92.00	72	72	76	58	76.00	80	80	79	76	76.00	80	80	79	76	76.00	84.00
10	100	100	100	100	100.00	89.06	89.06	89.06	89.06	89.06	94.53	94.53	94.53	94.53	89.06	94.53	94.53	94.53	94.53	94.53	94.53
11	75.82	72.53	79.49	81.32	97.80	55.31	53.11	56.41	59.71	72.89	65.57	62.82	67.95	70.51	72.89	65.57	62.82	67.95	70.51	72.89	85.35
12	92.86	91.43	95.71	75.71	100.00	64.29	70	77.14	75.71	92.86	78.57	80.71	86.43	75.71	92.86	78.57	80.71	86.43	75.71	92.86	96.43
13	100	100	100	98	100.00	90	90	91	85	92.00	95	95	95.50	91.50	92.00	95	95	95.50	91.50	92.00	96.00
14	90	90	82	86	96.00	90	88	86	80	86.00	90	89	84	83	86.00	90	89	84	83	86.00	91.00
15	83.67	81.63	87.76	85.71	95.92	73.47	71.43	67.35	71.43	63.27	78.57	76.53	77.55	78.57	63.27	78.57	76.53	77.55	78.57	63.27	79.59
<b>Mean</b>	85.88	85.11	85.60	86.58	<b>95.43</b>	78.94	79.71	80.83	74.08	<b>81.56</b>	82.41	82.41	83.21	80.33	<b>81.56</b>	82.41	82.41	83.21	80.33	<b>81.56</b>	<b>88.49</b>

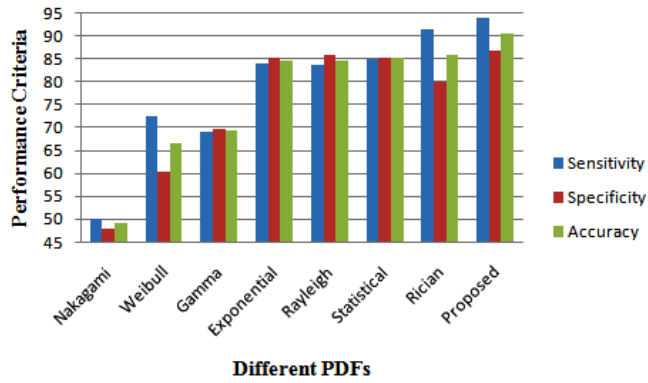


Figure 3.7: Variation profile of with-in frame feature is modeled with different PDFs and model parameters are used as input to classifiers. Mean of all the performance criteria are plotted for various PDFs

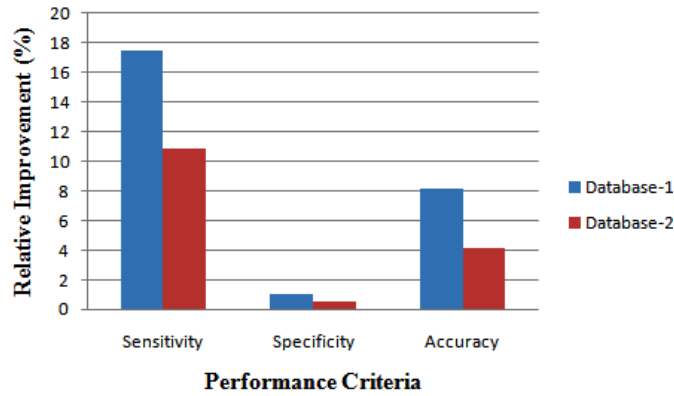


Figure 3.8: Relative Improvement with the proposed method comparing to the conventional approach. In the conventional approach, unlike sub-frame based analysis, entire frame is used for feature extraction and those are given as inputs directly to the classifier

input to classifier. The relative improvement achieved for both the datasets by the proposed approach with respect to the conventional approach is reported in Fig. 3.8. It is readily observable from the figure that there is relatively a large improvement in sensitivity and accuracy for both the databases.

Instead of modeling the within frame feature variation pattern, another alternative could be to model the data variation of the given frame. Pre-processed frame data are being subjected to the modeling and statistical analysis and the

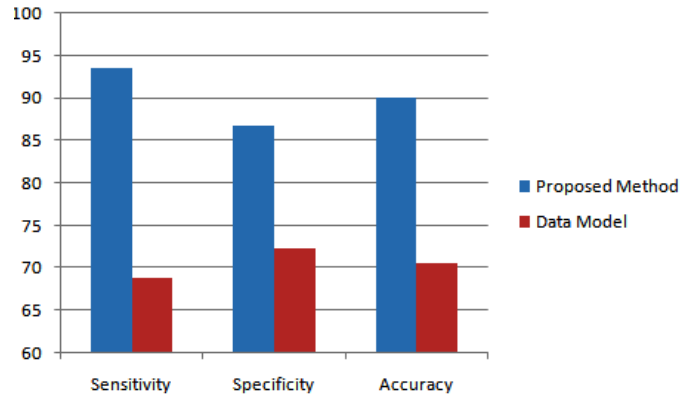


Figure 3.9: Comparison of Proposed Method with Data Modeling. In data modeling, unlike using the feature variation profile, modeling is applied on the pre-processed EEG data.

performance comparison of is made with the proposed method. The results are shown in Fig. 3.9. It is clearly shown from the figure that proposed method offers significant improvement than modeling the original pre-processed data.

It is generally regarded that most information in scalp EEG lies in low frequencies (less than 40Hz). However, recent study shows that neural activity extends far beyond the conventional frequency ranges. At high frequencies of EEG signal, rhythmic band activities are identified and it is shown that their properties depend on state of vigilance [35]. In this work, analysis is carried on with various numbers of IMFs. Figure 3.10 shows the accuracy of the proposed method using various number of modes. It is shown that utilization of higher frequency IMFs improve the overall result significantly. The number of modes above five have higher accuracies compared to the analyses with number of modes below five. It is also seen that analysis with five modes provides the best accuracy, which is recommended in this work. As it discussed in Section 3.1.2, number of modes below five provides low accuracy as they fail to encapsulate the higher frequency band and for the number of modes above five the accuracies are similar indicating redundant high frequency modes.

Table 3.4: Effect of model fitting on classification performance (results with and without using the proposed model fitting)

Method	Se.(%)	Sp.(%)	Acc.(%)	GSI
without modeling	65.33	65.02	65.17	0.69
Proposed Method	94	86.92	90.46	0.91

To show the effect of modeling, the proposed method is compared with the use of the extracted feature variation pattern as direct input to the classifier. It is revealed from Table 3.4 that the proposed method offers significantly better classification performance and GSI value. It shows the effectiveness of modeling and statistical analysis in quantifying the feature variation pattern and providing discriminative set of features.

Comparison of the proposed method is made with the existing methods for the subjects mentioned in Table 2.2 and the result is reported in Table 3.5. From the Table it is evident that the proposed method provides the better result compared to the existing methods. It can be seen that the performance of [15] is close to the proposed method. However, in [15] EEG signal is divided into sub-bands using

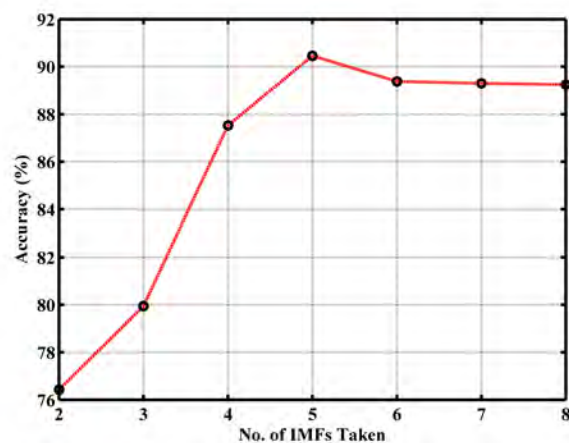


Figure 3.10: Classification Accuracy with different number of VMD modes taken

Table 3.5: Performance Comparison with the Methods Available in Literature

Method	Database-A			Database-B		
	Se.(%)	Sp.(%)	Acc.(%)	Se.(%)	Sp.(%)	Acc.(%)
[11]	65.74	59.15	62.45	60.30	56.50	58.40
[16]	77.69	79.96	78.83	72.143	66.46	69.302
[17]	81.47	83.28	82.38	80.084	80.647	80.366
[18]	72.40	70.31	71.36	71.62	69.88	70.75
[19]	78.4	76.3	77.35	76.62	74.88	75.75
[15]	93.7	83.61	88.65	94.2	80.41	87.31
<b>Proposed</b>	<b>94</b>	<b>86.92</b>	<b>90.46</b>	<b>95.43</b>	<b>81.56</b>	<b>88.49</b>

Table 3.6: Classification performance with all subjects combined

Cross-Validation	Sensitivity (%)	Specificity (%)	Accuracy (%)
leave-one-out	96.90	87.93	92.42
10-fold	97.18	87.72	92.36
5-fold	96.22	87.08	91.59
2-fold	96.39	85.95	91.17

fixed bandwidth bandpass which may fail to capture the variation in dominant frequencies from person to person, time to time due to changes neural activity which is discussed in Section 3.1.2. Moreover, unlike proposed method, high frequency ( $>40\text{Hz}$ ) EEG data are not taken for analysis.

In order to evaluate the performance of the proposed method, instead of subject specific analysis, one idea could be to apply cross-validation schemes on all frames from all subjects mentioned in Table 2.2 for [25] together. The result achieved for this approach is shown in Table 3.6. It is evident from the Table that the proposed method shows very satisfactory performance in classifying apnea and non-apnea frames.

EEG signals reflect the underlying cortical activation, and therefore different electrodes exhibit the distinct functional roles during sleep. According to the rec-

ommendations of Rechtschaffen and Kales [36], it requires one EEG lead with electrodes placed either at C4-A1 or C3-A2 according to the 10-20 system of electroencephalography electrodes placement on the skull. In agreement with this view the 2007 AASM Manual [37] recommended the use of three standard EEG electrodes for the scoring of sleep; including central, frontal and occipital electrodes. However, [38] showed that no differences are observed in arousal scoring statistics when only central electrode is used compared to using three electrodes (frontal, central, and occipital). In the proposed method, the databases used for apnea patients utilized different electrodes for data acquisition. The performance of apnea detection of the proposed method with respect to electrode position is presented in Table 3.7. It is interesting to note that the result very well supports the recommendation of Rechtschaffen and Kales. Here the electrodes with central position (C3-A2, C4-A1) have significantly better apnea detection performance compared to other positions.

Table 3.7: Effect of Position of Electrode in Apnea Detection

Electrode Position	No. of Subjects	Sensitivity (%)	Specificity (%)	Accuracy (%)
C4-A1	4	95.42	85.61	90.51
C3-A2	23	94	86.92	90.46
O2-A1	2	84.29	79.76	82.02
C3-O1	9	97.78	81.74	89.76

### Classifying Apnea Patients and Healthy Subjects

Here, non-apnea frames are taken from healthy subjects and the task of classifying apnea and healthy subjects is considered. Different cross-validation schemes are applied for performance evaluation and the details of the result are reported in Table 3.8. For each cross-validation scheme, average result of ten independent

trials is reported. From the Table it is evident that the proposed method achieves superior performances in classifying apnea and healthy subjects in terms of all performance criteria.

Table 3.8: Performance of the proposed method in classifying apnea and healthy subjects

<b>Cross-Validation</b>	<b>Sensitivity (%)</b>	<b>Specificity (%)</b>	<b>Accuracy (%)</b>
leave-one-out	98.83	97.55	98.19
10-fold	98.80	98.15	98.45
5-fold	98.82	97.73	98.27
2-fold	98.55	97.52	98.03

### 3.3 Conclusion

In this work, instead of considering the entire frame of given EEG data at a time, a unique sub-frame based VMD analysis is followed. VMD divides a signal into  $K$  band-limited intrinsic mode functions (BLIMFs) which are compact around a center frequency calculated solving a constrained variational problem. Such BLIMFs with adaptive center frequency can represent neural activity better compared to band limited EEG signal collected by bandpass filtering with definite center frequency and bandwidth. Moreover, it is shown that for EEG data, the number of VMD modes can be taken as five ensuring better result and limited computational complexity. Features expected to be discriminative for apnea detection are computed from each BLIMF of small duration sub-frame EEG data and temporal variation of features are generated for each mode. Unlike analysis over the entire frame, such small duration sub-frame based analysis and feature extraction can preserve local characteristics better. It is shown that if the extracted temporal feature variations are directly used for classification, it yields a poor result. Hence, modeling and statistical analysis are carried out on extracted feature

variation pattern, which provides an opportunity to characterize the amplitude variation of it. Among different PDF models, it is discovered that in terms of GSI Rician PDF offers the best feature quality. Unlike the established methods, the proposed is employed to classify apnea and non-apnea frames of an apnea patients as well as discriminate apnea and healthy subjects, which has a great demand in the field of diagnosis. The proposed method is evaluated on three different and large public databases of apnea patients with wide variation in AHI and healthy subjects and three different criteria of classification have been adopted to measure the effectiveness of the proposed method. In each of the cases, the proposed method offers significantly better classification performance in comparison to some existing methods in terms of sensitivity, specificity and accuracy. As a result, the proposed scheme can be employed in clinical applications to reduce the burden of the clinicians in apnea detection.



## Chapter 4

# Model Based Apnea Detection

## Using Wavelet Packet

## Decomposed EEG Signal

In this Chapter, an automatic sleep detection scheme using single lead EEG signal is proposed where analysis is carried on the wavelet domain. The given raw EEG frame is pre-processed and divided into overlapping sub-frames. Multi-level Wavelet Packet Decomposition is carried out on each sub-frame to extract EEG signals corresponding to different frequency bands. Instead of utilizing the wavelet packet coefficients directly for feature extraction, wavelet packet reconstruction at each node is carried out and features are calculated from the reconstructed signal. Wavelet preserves the best time-frequency resolution and hence, features calculated from them give the best estimate of the neural activities. Instead of directly using the extracted feature vector, within frame feature value variation pattern is modeled with a suitable characteristic probability distribution function (PDF) and the fitted model parameters are then used in K-NN classifier to classify apnea and non-apnea frames. Here, both classification scenarios- classifying apnea and

non-apnea frames in the data of an apnea patient and classification of apnea and healthy subjects, are taken into consideration. The experimentation is carried out in the same dataset used in Chapter 2.

## 4.1 Proposed Method

Each EEG frame is divided into multiple overlapping sub-frames and each sub-frame is divided into band limited signal using wavelet packet decomposition based reconstruction. Features are extracted from each band limited reconstructed signal and within frame feature variation pattern is constructed. Next, the within frame temporal feature variation pattern is modeled with characteristic probability density function (PDF) and the fitted parameters are used as final feature vector. Detailed description of the steps involved in the proposed method is presented in this section.

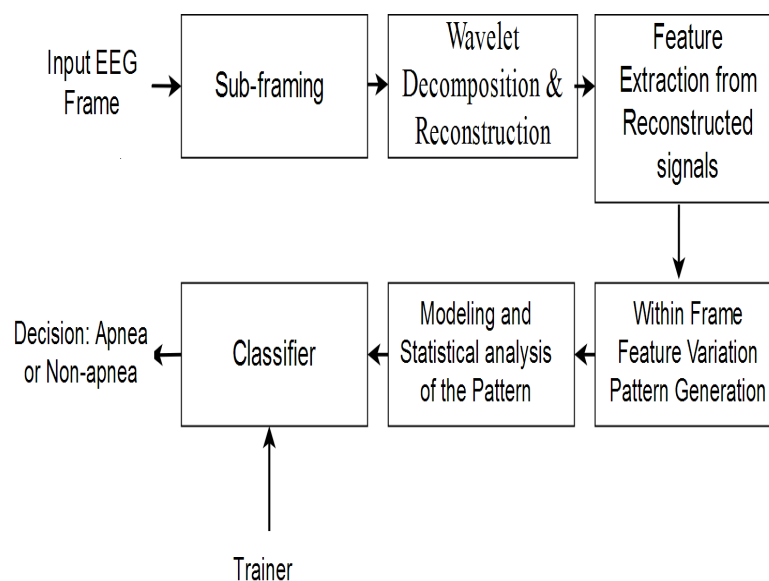


Figure 4.1: Flow chart of the Proposed method

Each given raw EEG frame is first pre-processed using dc offset removal, frame

amplitude normalization and energy normalization. Instead of carrying out analysis on the entire duration of the frame at a time, in this work, a sub-frame based analysis is adopted where the main frame is divided into a number smaller duration frames (these are called sub-frames) and a considerable amount of overlap is maintained between successive sub-frames. Sub-framing operation is carried out as like [15] where from an  $N$  length frame, with sub-frame duration  $M$  samples and shifting by  $p$  samples, a total  $\frac{N-M}{p} + 1$  number of sub-frames are obtained. Such sub-frame based analysis concentrates on smaller durations and hence it is expected to capture local information better. Moreover, as typically apnea duration is around 10s or so, only a portion of the main frame duration correspond to apnea. Hence, instead of working with the entire frame duration, it is beneficial to analyze shorter durations. % and develop an

#### **4.1.1 Wavelet Packet Decomposition**

Due to random nature of EEG data and interferences introduced during recording, it is very difficult to obtain distinctive characteristics from directly analyzing the time domain EEG data. In view of obtaining better distinguishing behavior of EEG signal, one common approach is to divide the EEG data in various frequency bands and then carry out analysis in each band separately. In different applications, EEG signal is divided into five frequency band-limited signals, namely- delta (0.25-4 Hz), theta (4-8 Hz), alpha (8-12 Hz), sigma (12-16 Hz) and beta (16-40 Hz), where the frequency bands are well established in literature and exhibit differences in frequency (Hz), amplitude and activity level. Delta, theta and alpha bands correspond to deep sleep, mild sleep and relax state, respectively while sigma and beta bands refer to alert states [32]- [33]. During apnea, as the breathing is paused, level of carbon dioxide rises in the bloodstream, which is recognized by the chemoreceptors. As a result, person sleeping is signaled by brain

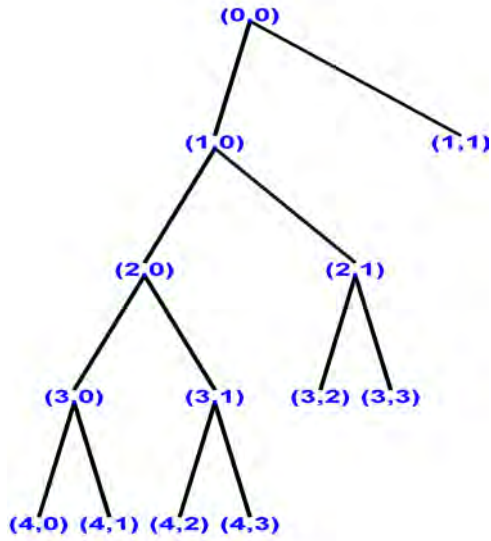


Figure 4.2: Tree decomposition of EEG signal

to breathe in air and wake up [23]. It is expected to have significant variation in different EEG frequency bands due to the above mentioned changes in neural activity from non-apnea to apnea. Hence, instead of carrying out analysis on the original frame, band limited analysis is followed in the proposed method.

In this work, to decompose each sub-frame of EEG data wavelet analysis is utilized. Wavelet decomposition (WD), the most common time-frequency multi-resolution technique, is found very effective in EEG [39]. However, WD based scheme performs decomposition only in the lower frequency bands. As an alternative, wavelet packet decomposition (WPD) can be utilized where decomposition is performed both in lower and higher frequency regions. Moreover, it offers low computational cost and ease of implementation [40], [41].

A wavelet packet is represented as a function [40], [41]

$$W_{\psi,k}^{\phi}(t) = 2^{-\psi/2}W^{\phi}(2^{-\psi}t - k), \phi = 1, 2, \dots, \psi^m \quad (4.1)$$

where parameters  $\phi$ ,  $\psi$ ,  $k$  and  $m$  correspond to modulation, dilation, translation and level of decomposition in wavelet packet tree respectively. The following relationships is utilized to obtain the wavelet  $W^\phi$  :

$$W^{2\phi} = \frac{1}{\sqrt{2}} \sum_{-\infty}^{\infty} h(k) W^\phi\left(\frac{t}{2} - k\right) \quad (4.2)$$

$$W^{2\phi+1} = \frac{1}{\sqrt{2}} \sum_{-\infty}^{\infty} g(k) W^\phi\left(\frac{t}{2} - k\right) \quad (4.3)$$

Here  $W^\phi$  is called as a mother wavelet and the discrete filters  $h(k)$  and  $g(k)$  are quadrature mirror filters associated with the scaling function and the mother wavelet function. The filtering operations in the WPD result in a change in the signal resolution and the sub-sampling operation causes change in the scale. Thus, WPD helps in analyzing the signal at different frequency bands with different resolutions.

The wavelet packet coefficients  $c_{\psi,k}^\phi$  corresponding to the signal  $y(t)$  can be obtained as,

$$c_{\psi,k}^\phi = \int_{-\infty}^{\infty} y(t) W_{\psi,k}^\phi(t) dt \quad (4.4)$$

provided the wavelet coefficients satisfy the orthogonality condition. Now, the EEG data can be decomposed to various levels. As the number of levels is increased, it is possible to extract band limited signals with smaller bandwidths, however, computational cost will increase in turn. As neural activity changes from non-apnea to apnea, it is preferable to consider both conventional low frequency bands as well as the high frequency band for analysis. In order to extract these frequency bands, the four level decomposition shown in 4.2 is used in the work. Here, node (1,1) represents the high frequency EEG band where (4,0), (4,1), (4,2), (4,3), (3,2) and (3,3) constitute the conventional low frequency bands. As EEG

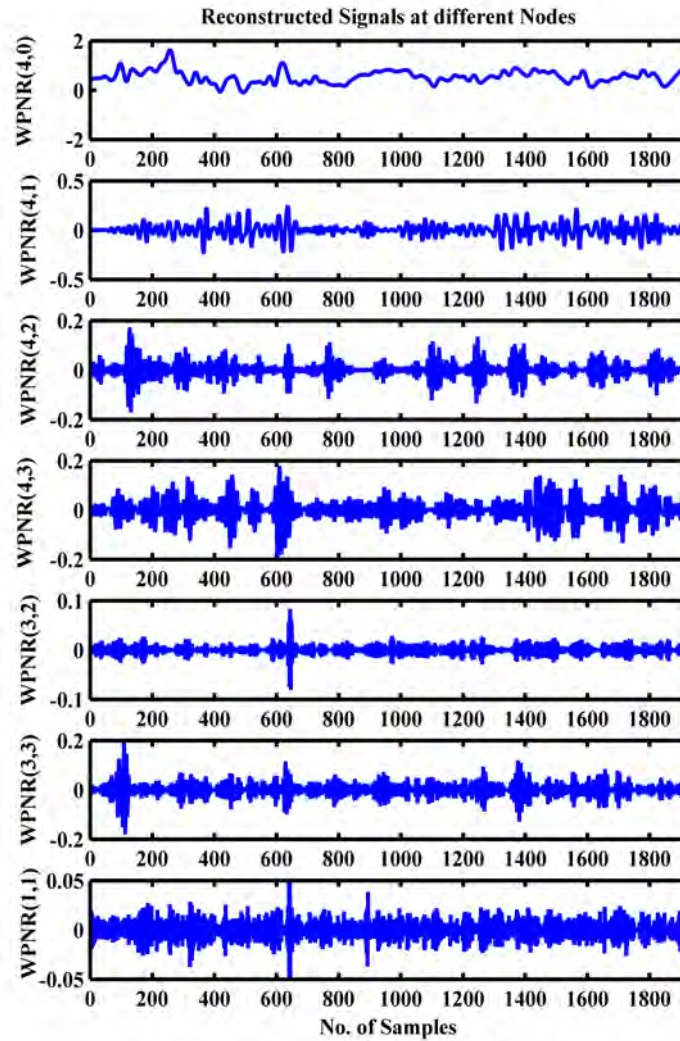


Figure 4.3: Wavelet packet reconstructed signals at different nodes

data mostly have significant information lying in lower bands, further decomposition of node (1,1) is not carried out which would have increased computational time and cost.

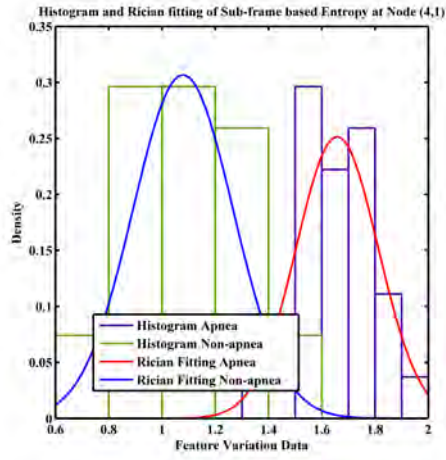
One major problem in WPD is the reduction of the length of wavelet coefficients in each decomposition level similar to conventional wavelet analysis. As a result,

if features are extracted from multi-level wavelet coefficients, there is a chance of getting deteriorated feature quality due to the reduced length of the coefficients in comparison to main data length. For example, for the four level decomposition shown in Fig. 4.2, the length of the WPD coefficients at the fourth level will be 1/16th of the main data length. To counter this problem, an approach can be to reconstruct signal at a particular node using the WPD coefficients of that node, which is named as WPNR. This reconstructed signal will represent the band limited version of the original signal and will have same length as the original signal. To demonstrate this, corresponding to the decomposition presented at Fig. 4.2, reconstructed signals at different nodes are shown in Fig. 4.3. It is to be seen that all the reconstructed signals have same length and they vary in terms of frequency content and amplitude. If WPNR signal at each node is considered for feature extraction, better statistical characteristics is expected as there is no reduction of length.

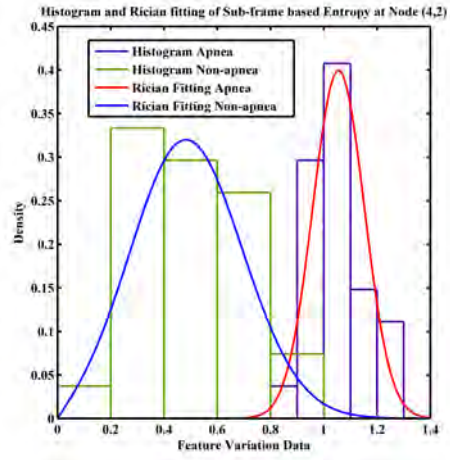
A large number of wavelet functions are available in the literature namely Daubechies, Symlets, Coiflet, BiorSplines, ReverseBior, and Discrete Meyer. Out of these, sym9 wavelet of the Symlets family is utilized in the Proposed Method.

#### **4.1.2 Modeling Analysis of Wavelet Packet Reconstructed Signal**

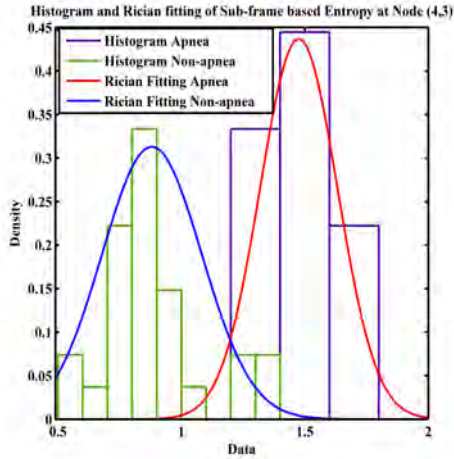
Each sub-frame based WPNR signal is statistically analyzed where statistical features are calculated from each of the WPNR signals. Since EEG signal contains information regarding different mental and motor-imagery states of the brain, it is expected that for a person at sleep, during apnea events, there will be certainly a rapid change in information content in EEG recordings. Moreover, variation in EEG data increases during apnea than non-apnea instances. Such changes in information content. In order to capture the changes, in the proposed method, en-



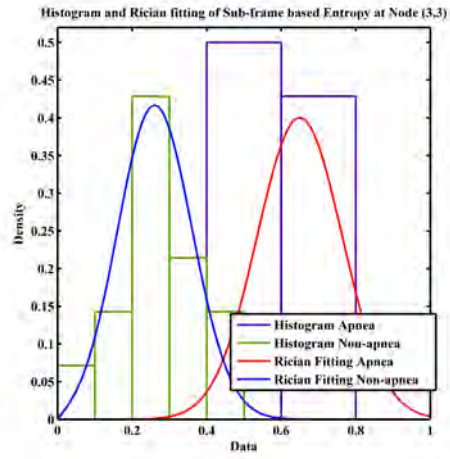
(a)



(b)



(c)



(d)

Figure 4.4: Test frame is divided into multiple sub-frames and each sub-frame is wavelet packet decomposed. Wavelet coefficients at each node are reconstructed using wavelet packet reconstruction (WPNR). Entropy and log-variance are calculated from each WPNR signal. Histograms of the calculated feature variation patterns of entropy and the corresponding Rician fittings of various WPNR signals are shown for both apnea and non-apnea frames.

entropy and logarithm of variance (LV) are chosen as features to be extracted from each sub-frame based WPNR signal.

As there are multiple sub-frames within a frame, features are calculated for



multiple times for same node but for different sub-frames. Hence, it gives an opportunity to obtain a within frame feature variation profile of a particular feature for each node. If there are  $W$  number of sub-frames, the within frame feature variation pattern for  $k$ th node can be generated as

$$\textit{Variation Pattern} = [F_{1k}, F_{2k}, F_{3k}, \dots, F_{Wk}], \quad (4.5)$$

where  $F_{Wk}$  denotes the feature calculated from the  $k$ th node of the  $W$ th sub-frame.

In order to represent the within frame feature variation pattern for different WPNR signals, in Fig. 4.5, entropy values calculated for each sub-frame based WPNR signal are presented for both apnea and non-apnea. It is evident from the figure that in different modes, characteristics of feature variation is different from apnea to non-apnea.

Instead of directly using the calculated sub-frame based features for classification, which will increase feature dimension and computational time, the extracted feature variation patterns are further subjected to model fitting as like [15]. For modeling, feature variation pattern of each WPNR signal is fitted with suitable PDF and the fitted parameters are used as features. The formation of final feature vector ( $\mathbf{F}$ ) is shown in (4.6). Among different PDFs, in this work, Rician PDF is used and in Fig. 4.4, for both apnea and non-apnea, Rician fittings of feature variation patterns for different WPNR signals are shown. It is evident from the figure that the fitted Rician PDFs for apnea and non-apnea frames differ widely and there are minimum overlap between the two. Hence the fitted parameters are expected to show good classification performance in differentiating two classes.

$$\mathbf{F} = [\mathbf{F}_{wpd,1} \ \mathbf{F}_{wpd,2} \ \dots \ \mathbf{F}_{wpd,n}] \quad (4.6)$$

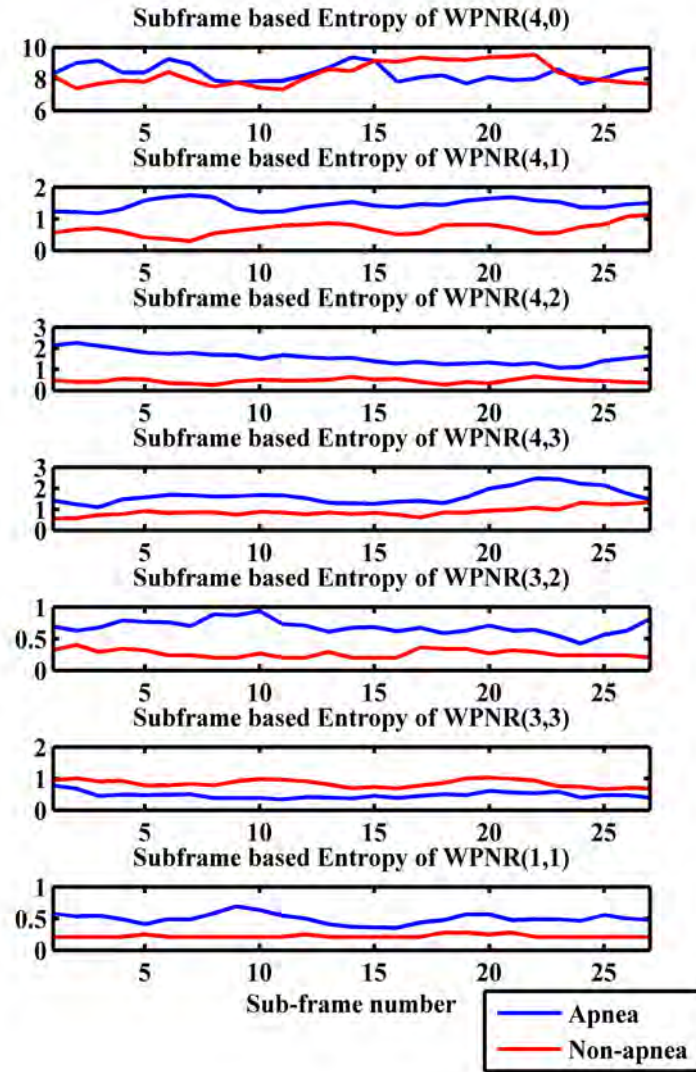


Figure 4.5: Wavelet packet reconstructed signals at different nodes

## 4.2 Results and Discussions

This section presents the description of the databases used, the detailed analysis on the feature quality of the extracted features and the classification results of sleep apnea detection.

### 4.2.1 Database

For the purpose of experimentation, subjects mentioned in Table 2.2 in Chapter 2 are used in this work. For [25] and [26], frame durations taken are 15s and 30s, respectively, depending on the respective ground truths. There are two considerations to make in selection of sub-frame duration and the size of overlap. A big sub-frame length with large overlap will not provide enough data for feature variation pattern and thus the corresponding model fitting will be biased. On the other hand, a very small sub-frame length with large overlap is an option but very short sub-frame length might provide incorrect estimate of features, such as entropy and log-variance. Moreover, large overlap between consecutive sub-frames will result into a large number of feature variation data that will increase the computational complexity. Hence, keeping both the issues in consideration, in this work a moderate sub-frame length of 2s and 4s are used for databases- [25] and [26], respectively and 80% overlap between two successive sub-frames are maintained to ensure enough data points for model fitting with moderate computational complexity.

### 4.2.2 Classification Result

For the classification purpose, there are two cases to consider- (i) apnea and non-apnea classification in the data of apnea patients and (ii) apnea patients and healthy subjects classification. In K-NN classifier, cosine distance function and  $K$  equal to 9 are chosen. Standard performance measures described in (2.11)-(2.13) are used to evaluate the performance of the proposed method. The definition of the accuracy measures such as TP,TN,FP,FN, are provided in Table 2.6.

Table 4.1: Performance analysis of the proposed method for various PDF fitting using leave-one-out cross validation (database-A)

S/No	Sensitivity(%)			Specificity(%)			Accuracy(%)					
	Exp.	Ray.	Normal	Rician	Exp.	Ray.	Normal	Rician	Exp.	Ray.	Normal	Rician
1	78.99	76.47	77.31	95.80	78.99	75.63	78.15	80.67	78.99	76.05	77.73	88.24
2	93.51	90.84	93.89	98.09	97.71	96.18	96.95	96.56	95.61	93.51	95.42	97.33
3	73.08	73.08	80.77	92.31	84.62	78.85	86.54	88.46	78.85	75.96	83.65	90.38
4	83.78	77.03	83.78	94.59	89.19	83.78	86.49	85.14	86.49	80.41	85.14	89.86
5	77.46	76.06	78.87	88.73	87.32	78.87	91.55	90.14	82.39	77.46	85.21	89.44
6	68.33	70.00	61.67	98.33	85	80	81.67	85	76.67	75	71.67	91.67
7	97.53	96.91	98.77	100	90.74	91.36	90.74	88.27	94.14	94.14	94.75	94.14
8	89.66	89.66	79.31	96.55	96.55	96.55	100.00	93.10	93.10	93.10	89.66	94.83
9	94.27	88.02	95.31	98.44	91.67	85.94	92.71	90.63	92.97	86.98	94.01	94.53
10	89.09	87.27	83.64	92.73	85.45	81.82	81.82	80	87.27	84.55	82.73	86.36
11	94.71	93.27	94.71	97.60	96.15	95.67	93.75	92.31	95.43	94.47	94.23	94.95
12	96.08	96.08	96.08	98.04	100	100	100	100	98.04	98.04	98.04	99.02
13	100	100	100	100	88.89	88.89	88.89	88.89	94.44	94.44	94.44	94.44
14	96.15	94.87	94.87	100	100	100	100	94.87	98.08	97.44	97.44	97.44
15	90.91	93.94	92.42	96.97	81.82	80.30	80.30	83.33	86.36	87.12	86.36	90.15
16	83.61	86.89	85.25	96.72	88.52	90.16	90.16	90.16	86.07	88.52	87.70	93.44
17	94.74	89.47	89.47	100	84.21	89.47	84.21	84.21	89.47	89.47	86.84	92.11
18	81.56	82.27	78.72	96.45	79.43	76.60	80.14	80.85	80.50	79.43	79.43	88.65
19	96.15	95.38	96.92	100	93.08	93.85	94.62	96.15	94.62	94.62	95.77	98.08
20	100	100	97.50	97.50	90	90	90	90	95	95	93.75	93.75
21	87.50	83.75	86.25	97.50	93.75	90	92.50	85	90.63	86.88	89.38	91.25
22	88.68	83.96	88.21	99.06	74.53	74.53	81.13	87.74	81.60	79.25	84.67	93.40
23	91.67	84.62	92.31	98.08	85.26	79.49	83.97	87.18	88.46	82.05	88.14	92.63
<b>Mean</b>	89.02	87.38	88.09	<b>97.11</b>	88.82	86.87	88.97	<b>88.64</b>	88.92	87.13	88.53	<b>92.87</b>

Table 4.2: Performance analysis of the proposed method for various PDF fitting (Database-B)

S/No	Sensitivity(%)				Specificity(%)				Accuracy(%)			
	Exp.	Ray.	Normal	Rician	Exp.	Ray.	Normal	Rician	Exp.	Ray.	Normal	Rician
1	89.19	94.59	89.19	91.89	86.49	89.19	89.19	86.49	87.84	91.89	89.19	89.19
2	75.38	72.31	78.46	96.92	84.62	86.15	83.08	84.62	80.00	79.23	80.77	90.77
3	77.78	75.56	82.22	94.44	88.89	85.56	92.22	87.78	83.33	80.56	87.22	91.11
4	83.33	83.33	71.43	85.71	85.71	85.71	83.33	80.95	84.52	84.52	77.38	83.33
5	74.87	74.35	75.92	100	81.68	78.01	82.20	81.68	78.27	76.18	79.06	90.84
6	93.04	91.30	94.35	100	75.65	73.48	76.52	87.39	84.35	82.39	85.43	93.70
7	89.07	86.34	91.80	99.45	77.60	75.96	76.50	89.62	83.33	81.15	84.15	94.54
8	86.52	80.85	83.69	100	78.01	78.01	73.05	78.72	82.27	79.43	78.37	89.36
9	92	92	90	98	84	88	84	88.00	88	90	87	93
10	98.53	100	100	100	89.71	89.71	89.71	89.71	94.12	94.85	94.85	94.85
11	75.82	75.82	72.53	98.53	53.11	57.51	50.55	77.29	64.47	66.67	61.54	87.91
12	91.43	92.86	90	100	80	84.29	78.57	92.86	85.71	88.57	84.29	96.43
13	99	99	99	100	88	87	89	91	93.5	93	94	95.50
14	92	84	84	100	90	90	94	86	91	87	89	93
15	84	86	88	100	62	60	72	74	73	73	80	87
<b>Mean</b>	86.80	85.89	86.04	<b>97.66</b>	80.36	80.57	80.93	<b>85.07</b>	83.58	83.23	83.48	<b>91.37</b>

## Classification of Apnea and Non-apnea Frames in the data of Apnea Patients

Here two classes, apnea and non-apnea, both come from the data of apnea patients. Healthy subjects are considered in another section. The proposed method is evaluated for different PDFs and detailed result is shown in in Tables 4.1 and 4.2 for both the databases utilizing leave-one-out cross-validation scheme. Out of several PDFs, it is evident that Rician PDF offers the best result in terms of each of the performance criteria. The improvement in specificity with Rician in comparison to other PDFs is moderate whereas the sensitivity and accuracy values are far superior. Hence, in this work, Rician PDF is proposed for fitting the feature variation data. In Tables 4.1 and 4.2, subject specific results have been reported where test and train contain data from the same subject. However, another alternative could be to mix data from all the subjects together and apply different cross-validation schemes on them. Table 4.3 shows the result of the analysis and it can be seen that in all the cross-validation schemes the result is consistent.

Table 4.3: Classification performance with all subjects combined of database-A

Cross-validation schemes	Sensitivity	Specificity	Accuracy
Leave one out	98.54	85.82	92.18
10-fold	99.15	84.56	91.97
5-fold	98.73	84.42	91.67
2-fold	98.73	82.88	90.87

In the proposed features are calculated from the reconstructed signal which is named as WPNR. However, instead of using wavelet reconstruction, one alternative could be to extract features from the coefficients and later on model these sub-frame based features. A comparison between these two in terms of classification result is presented in Table 4.4 and it is shown that utilization of reconstructed

Table 4.4: Comparison of the Proposed method with using Wavelet coefficients for modeling

Method	Se.	Spe.	Acc.
Coefficient Modeling	96.806	81.896	89.35
<b>Proposed</b>	<b>97.11</b>	<b>88.64</b>	<b>92.87</b>

signal improves the performance. The reason for this is that with more level of decomposition the number of data points gets lesser, hence in the deeper levels the number of data point is much lesser. As a consequence, the statistical features calculated from the shorter length coefficients might not provide the correct estimate. In reconstruction the length remains unchanged hence no such problem occurs.

In the Proposed method four level wavelet packet decomposition is considered. The classification result with various levels of decomposition is shown in Fig. 4.6. It is seen that four level decomposition gives the best result in terms of every performance criterion.

Comparison of the proposed method is made with the existing methods for the subjects mentioned in Table 2.2 and the result is reported in Table 4.5. From the

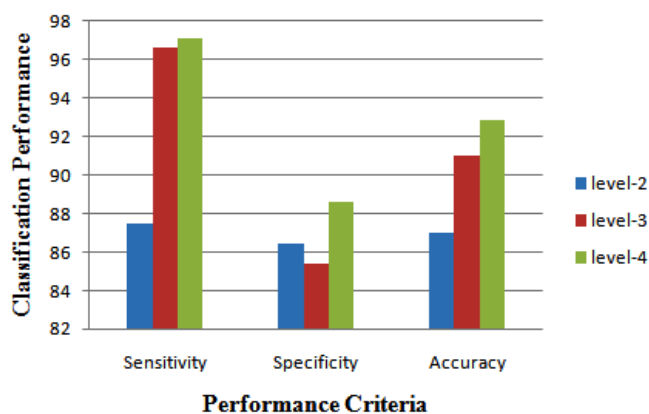


Figure 4.6: Classification Result with Various Levels of Decomposition

Table 4.5: Performance Comparison with the Methods Available in Literature

Method	Database-A			Database-B		
	Se.(%)	Sp.(%)	Acc.(%)	Se.(%)	Sp.(%)	Acc.(%)
[11]	65.74	59.15	62.45	60.30	56.50	58.40
[16]	77.69	79.96	78.83	72.143	66.46	69.302
[17]	81.47	83.28	82.38	80.084	80.647	80.366
[18]	72.40	70.31	71.36	71.62	69.88	70.75
[19]	78.4	76.3	77.35	76.62	74.88	75.75
[15]	93.7	83.61	88.65	94.2	80.41	87.31
<b>Proposed</b>	<b>97.11</b>	<b>88.64</b>	<b>92.87</b>	<b>97.66</b>	<b>85.07</b>	<b>91.37</b>

Table it is evident that the proposed method provides the better result compared to the existing methods.

### Classifying Apnea Patients and Healthy Subjects

Here, non-apnea frames are taken from healthy subjects and the task of classifying apnea and healthy subjects is considered. Different cross-validation schemes are applied for performance evaluation and details of the result are reported in Table 4.6. For each cross-validation scheme, average result of ten independent trials is reported. From the Table it is evident that the proposed method achieves superior performances in classifying apnea and healthy subjects in terms of all performance criteria.

Table 4.6: Performance of the Proposed Method in classifying apnea and healthy subjects

Cross-validation schemes	Sensitivity (%)	Specificity (%)	Accuracy (%)
Leave one out	99.91	99.57	99.74
10-fold	100	99.35	99.68
5-fold	99.94	99.44	99.69
2-fold	99.91	99.39	99.65



### 4.3 Conclusion

In this work, instead of analyzing the given whole duration EEG data at a time, a sub-frame based WPD analysis is carried out. WPD allows to extract band limited EEG signals with high time-frequency resolution. Moreover, in this work, instead of working with the wavelet coefficients, wavelet packet reconstruction is introduced which, unlike wavelet coefficients, has same length as the original signal. Wavelet analysis is carried out on sub-framed EEG data to extract the conventional band limited EEG signals and features are calculated from the reconstructed signals. Such use of sub-framing provides an opportunity of generating temporal variation of the extracted feature within the frame. Next, model fitting is carried out on the resulting feature variation pattern, which gives an opportunity to utilize both local and global characteristics of a frame. Among various PDF models, it is found that the Rician PDF is offering the best classification performance in all three databases. In each of the cases, the proposed method offers significantly better classification performance in comparison to some existing methods in terms of sensitivity, specificity and accuracy. The proposed method can not only classify apnea patient and healthy subject but also classify apnea and non-apnea frames of an apnea patient, which has a great demand in the overnight polysomnography (PSG) to reduce human error, labor and cost. It makes the proposed method to be widely applicable in a greater domain of diagnosis.

In this work, instead of considering the entire frame of given EEG data at a time, a unique sub-frame based VMD analysis is followed. VMD divides a signal into  $K$  band-limited intrinsic mode functions (BLIMFs) which are compact around a center frequency calculated solving a constrained variational problem. Such BLIMFs with adaptive center frequency can represent neural activity better compared to band limited EEG signal collected by bandpass filtering with definite center frequency and bandwidth. Moreover, it is shown that for EEG data, the

number of VMD modes can be taken as five ensuring better result and limited computational complexity. Features expected to be discriminative for apnea detection are computed from each BLIMF of small duration sub-frame EEG data and temporal variation of features are generated for each mode. Unlike analysis over the entire frame, such small duration sub-frame based analysis and feature extraction can preserve local characteristics better. It is shown that if the extracted temporal feature variations are directly used for classification, it yields a poor result. Hence, modeling and statistical analysis are carried out on extracted feature variation pattern, which provides an opportunity to characterize the amplitude variation of it. Among different PDF models, it is discovered that in terms of GSRician PDF offers the best feature quality. Unlike the established methods, the proposed is employed to classify apnea and non-apnea frames of an apnea patients as well as discriminate apnea and healthy subjects, which has a great demand in the field of diagnosis. The proposed method is evaluated on three different and large public databases of apnea patients with wide variation in AHI and healthy subjects and three different criteria of classification have been adopted to measure the effectiveness of the proposed method. In each of the cases, the proposed method offers significantly better classification performance in comparison to some existing methods in terms of sensitivity, specificity and accuracy. As a result, the proposed scheme can be employed in clinical applications to reduce the burden of the clinicians in apnea detection.

# Chapter 5

## Conclusion

### 5.1 Concluding Remarks

In this thesis, Rician model based sleep apnea detection schemes are presented in three different domains. Instead of utilizing the entire EEG frame, sub-frame based analysis has been carried out which gives an opportunity to better extract the local information. Different time-frequency domains, such as multi-band EEG signals, variational mode decomposed EEG signal, wavelet packet reconstructed EEG signal have been used since such band limited signals in different domains can encapsulate neural activities better and thus a difference in terms of neural activity from non-apnea to apnea can be exploited. Statistical features, such as entropy and log-variance have been extracted from each sub-frame and thus within frame feature variation patterns for every band limited signals can be generated. It is shown that Rician modeling and use of the fitted Rician parameters as feature can provide high accuracy in apnea detection in all the domains. Detailed analyses and various types of investigation carried out on three different publicly available databases verify that the proposed model based sleep apnea detection schemes are capable of detecting sleep apnea frames in the data of apnea patients and

classifying apnea and healthy subjects with high accuracy.

## 5.2 Contribution of this Thesis

The major contribution of the thesis are summarized below:

- Most of the apnea detection methods available in literature utilize combination of multiple physiological signals, such as ECG, EEG, EMG, EOG, and nasal pressure. Such use of multiple signals has several disadvantages. Instead of using multiple signals, the this work focuses on using single channel EEG signal for apnea detection which is very rare in literature.

- Proposed method fits probabilistic model in temporal feature variation pattern extracted from band limited EEG signals. For the first time within frame feature variation pattern in various time-frequency domains are investigated and are fitted with probabilistic models. In the proposed method effect of various models are analyzed and a model is proposed. The performance of the proposed model fitting is not only judged by classification results but also by the theoretical feature quality tests.

- Other than working with strict frequency boundary based band limited signal, analysis is also carried on decomposed EEG signal to capture the behavior of multi-neural firing. Hence, variational mode decomposition (VMD) is used which can offer band limited intrinsic mode functions with adaptive center frequency. This variable center frequency allows to reflect the person to person changes in neural activity. Such VMD analysis in apnea detection is considered for the first time.

- In order to analyze the precise time frequency behavior for sub-frame based entropy-energy features, wavelet domain analysis is carried out which ensures better time frequency resolution. Modeling of within frame statistical feature variation in wavelet domain is attempted for the first time in apnea detection.

- Most of the existing work classifies apnea and healthy subjects. In the proposed work, both apnea and healthy subject classification and classification of apnea and non-apnea frames in the data of an apnea patient are carried out.

### **5.3 Scopes for Future Work**

In this thesis, three model based approaches have been developed for automatic detection of apnea frames, which will assist the clinicians in diagnosis. However, further classification of the detected apnea frames to one of its different types has not been considered. Moreover, the methods presented here work with offline data whereas future researches are required for real time apnea detection.

# Bibliography

- [1] Chamara V Senaratna, Jennifer L Perret, Caroline J Lodge, Adrian J Lowe, Brittany E Campbell, Melanie C Matheson, Garun S Hamilton, and Shyamali C Dharmage. Prevalence of obstructive sleep apnea in the general population: a systematic review. *Sleep medicine reviews*, 34:70–81, 2017.
- [2] Terri E Weaver and Charles FP George. Cognition and performance in patients with obstructive sleep apnea. In *Principles and Practice of Sleep Medicine: Fifth Edition*. Elsevier Inc., 2010.
- [3] Paul E Peppard, Terry Young, Mari Palta, and James Skatrud. Prospective study of the association between sleep-disordered breathing and hypertension. *New England Journal of Medicine*, 342(19):1378–1384, 2000.
- [4] Eyal Shahar, Coralyn W Whitney, Susan REdline, Elisa T Lee, Anne B Newman, F Javier Nieto, GEORGE T O’CONNOR, Lori L Boland, Joseph E Schwartz, and Jonathan M Samet. Sleep-disordered breathing and cardiovascular disease: cross-sectional results of the sleep heart health study. *American Journal of Respiratory and Critical Care Medicine*, 163(1):19–25, 2001.
- [5] Haitham M Al-Angari and Alan V Sahakian. Automated recognition of obstructive sleep apnea syndrome using support vector machine classifier. *IEEE Transactions on Information Technology in Biomedicine*, 16(3):463–468, 2012.

- [6] Jonathan A Waxman, Daniel Graupe, and David W Carley. Automated prediction of apnea and hypopnea, using a LAMSTAR artificial neural network. *American Journal of Respiratory and Critical Care Medicine*, 181(7):727–733, 2010.
- [7] Daniel Alvarez, Roberto Hornero, J Victor Marcos, Felix del Campo, and Miguel Lopez. Spectral analysis of electroencephalogram and oximetric signals in obstructive sleep apnea diagnosis. In *Proc. IEEE Annual International Conference of Engineering in Medicine and Biology Society, EMBC 2009.*, pages 400–403.
- [8] Derong Liu, Zhongyu Pang, and Stephen R Lloyd. A neural network method for detection of obstructive sleep apnea and narcolepsy based on pupil size and EEG. *IEEE Transactions on Neural Networks*, 19(2):308–318, 2008.
- [9] Md Riyasat Azim, Shah Ahsanul Haque, Md Shahedul Amin, and Tahmid Latif. Analysis of EEG and EMG signals for detection of sleep disordered breathing events. In *Proc. IEEE International Conference on Electrical and Computer Engineering (ICECE), 2010.*
- [10] Tim Schlüter and Stefan Conrad. An approach for automatic sleep stage scoring and apnea-hypopnea detection. *Frontiers of Computer Science*, 6(2):230–241, 2012.
- [11] Jing Zhou, Xiao-ming Wu, and Wei-jie Zeng. Automatic detection of sleep apnea based on EEG detrended fluctuation analysis and support vector machine. *Journal of Clinical Monitoring and Computing*, 29(6):767–772, 2015.
- [12] Robert Lin, Ren-Guey Lee, Chwan-Lu Tseng, Heng-Kuan Zhou, Chih-Feng Chao, and Joe-Air Jiang. A new approach for identifying sleep apnea syn-

- drome using wavelet transform and neural networks. *Biomedical Engineering: Applications, Basis and Communications*, 18(03):138–143, 2006.
- [13] Ren-Guey Lee, Chun-Chang Chen, Chun-Chieh Hsiao, Hsi-Wen Wang, and Ming-Shen Wei. Sleep apnea syndrome recognition using the GreyART network. *Biomedical Engineering: Applications, Basis and Communications*, 23(03):163–172, 2011.
- [14] S Taran, V Bajaj, and D Sharma. Robust Hermite decomposition algorithm for classification of sleep apnea EEG signals. *Electronics Letters*, 53(17):1182–1184, 2017.
- [15] Arnab Bhattacharjee, Suvasish Saha, Shaikh Anowarul Fattah, Wei-Ping Zhu, and M Omair Ahmad. Sleep apnea detection based on Rician Modeling of Feature Variation in Multi-band EEG Signal. *IEEE journal of biomedical and health informatics*, 2018.
- [16] Wafaa S Almuhammadi, Khald AI Aboalayon, and Miad Faezipour. Efficient obstructive sleep apnea classification based on EEG signals. In *Proc. IEEE Systems, Applications and Technology Conference (LISAT), 2015*.
- [17] Suvasish Saha, Arnab Bhattacharjee, Md Abu Aeioub Ansary, and SA Fattah. An approach for automatic sleep apnea detection based on entropy of multi-band EEG signal. In *Proc. IEEE Region 10 Conference (TENCON), 2016*, pages 420–423.
- [18] Celia Shahnaz, Ahmed Tahseen Minhaz, and Sk Tanvir Ahamed. Sub-frame based apnea detection exploiting delta band power ratio extracted from EEG signals. In *Proc. IEEE Region 10 Conference (TENCON), 2016*, pages 190–193.



- [19] Farhin Ahmed, Projna Paromita, Arnab Bhattacharjee, Suvasish Saha, Samee Azad, and SA Fattah. Detection of sleep apnea using sub-frame based temporal variation of energy in beta band in EEG. In *Proc. IEEE International WIE Conference on Electrical and Computer Engineering (WIECON-ECE), 2016*, pages 258–261.
- [20] Sachin Taran, Varun Bajaj, and Dheeraj Sharma. Teo separated AM-FM components for identification of apnea EEG signals. In *Proc. IEEE 2nd International Conference on Signal and Image Processing (ICSIP), 2017*, pages 391–395.
- [21] M Emin Tagluk and Necmettin Sezgin. A new approach for estimation of obstructive sleep apnea syndrome. *Expert Systems with Applications*, 38(5):5346–5351, 2011.
- [22] Chien-Chang Hsu and Ping-Ta Shih. A novel sleep apnea detection system in electroencephalogram using frequency variation. *Expert Systems with Applications*, 38(5):6014–6024, 2011.
- [23] Cristian Rotariu, Ciprian Cristea, Dragos Arotaritei, Radu G Bozomitu, and Alexandru Pasarica. Continuous respiratory monitoring device for detection of sleep apnea episodes. In *IEEE International Symposium for Design and Technology in Electronic Packaging (SIITME), 2016*, pages 106–109.
- [24] Athanasios Papoulis and S Unnikrishna Pillai. *Probability, Random Variables and Stochastic Processes*. Tata McGraw-Hill Education, fourth edition, 2002.
- [25] St. Vincent’s University Hospital / University College Dublin Sleep Apnea Database. URL: <http://www.physionet.org/physiobank/database/ucddb/>.

- [26] MIT-BIH Polysomnographic Database. URL: <https://www.physionet.org/physiobank/database/slpdb/>.
- [27] Sleep Recordings and Hypnograms in European Data Format (EDF). URL: <https://physionet.org/pn4/sleep-edfx/>.
- [28] Anil Bhattacharyya. On a measure of divergence between two statistical populations defined by their probability distribution. *Bull. Calcutta Math. Soc*, 1943.
- [29] John Greene. Feature subset selection using Thornton’s separability index and its applicability to a number of sparse proximity-based classifiers. In *Proc. Annual Symposium of the Pattern Recognition Association of South Africa*, 2001.
- [30] Sudhansu Chokroverty. *Sleep Disorders Medicine: Basic Science, Technical Considerations and Clinical Aspects*. Butterworth-Heinemann, 2013.
- [31] Konstantin Dragomiretskiy and Dominique Zosso. Variational mode decomposition. *IEEE transactions on signal processing*, 62(3):531–544, 2014.
- [32] Ernst Niedermeyer and FH Lopes da Silva. *Electroencephalography: basic principles, clinical applications, and related fields*. Lippincott Williams & Wilkins, 2005.
- [33] Wolfgang Klimesch. EEG alpha and theta oscillations reflect cognitive and memory performance: A review and analysis. *Brain research reviews*, 29(2-3):169–195, 1999.
- [34] Jiawei Han, Micheline Kamber, and Jian Pei. *Data Mining: Concepts and Techniques*. Elsevier, 2011.

- [35] Steven X Moffett, Sean M O'Malley, Shushuang Man, Dawei Hong, and Joseph V Martin. Dynamics of high frequency brain activity. *Scientific Reports*, 7(1):15758, 2017.
- [36] Sleep Computing Committee of the Japanese Society of Sleep Research Society (JSSR):, Tadao Hori, Yoshio Sugita, Einosuke Koga, Shuichiro Shirakawa, Katuhiro Inoue, Sunao Uchida, Hiroo Kuwahara, Masako Kousaka, Toshinori Kobayashi, et al. Proposed supplements and amendments to ‘a manual of standardized terminology, techniques and scoring system for sleep stages of human subjects’, the Rechtschaffen & Kales (1968) standard. *Psychiatry and clinical neurosciences*, 55(3):305–310, 2001.
- [37] Richard B Berry, Rita Brooks, Charlene E Gamaldo, Susan M Harding, CL Marcus, BV Vaughn, et al. The AASM manual for the scoring of sleep and associated events. *Rules, Terminology and Technical Specifications, Darien, Illinois, American Academy of Sleep Medicine*, 2012.
- [38] Warren R Ruehland, Fergal J O'Donoghue, Robert J Pierce, Andrew T Thornton, Parmjit Singh, Janet M Copland, Bronwyn Stevens, and Peter D Rochford. The 2007 AASM recommendations for EEG electrode placement in polysomnography: impact on sleep and cortical arousal scoring. *Sleep*, 34(1):73–81, 2011.
- [39] Akshansh Gupta, RK Agrawal, and Baljeet Kaur. Performance enhancement of mental task classification using EEG signal: a study of multivariate feature selection methods. *Soft Computing*, 19(10):2799–2812, 2015.
- [40] Deng Wang, Duoqian Miao, and Chen Xie. Best basis-based wavelet packet entropy feature extraction and hierarchical EEG classification for epileptic detection. *Expert Systems with Applications*, 38(11):14314–14320, 2011.

- [41] Xiaoou Li, Xun Chen, Yuning Yan, Wenshi Wei, and Z Jane Wang. Classification of EEG signals using a multiple kernel learning support vector machine. *Sensors*, 14(7):12784–12802, 2014.